i. Celecoxib inhibits mitochondrial O_2 consumption, promoting ROS dependent death of murine and human metastatic cancer cells via the apoptotic signalling pathway.

ii. Running Title: Celecoxib, mitochondrial ROS and cancer cell death.

iii. Rhys Pritchard,[1] Sara Rodríguez-Enríquez,[2] Silvia Cecelia Pacheco-Velázquez,[2] Vuk Bortnik,[1] Rafael Moreno-Sánchez,[2] and Stephen Ralph[1]

iv. [1]Menzies Health Institute Queensland, School of Medical Science, Griffith University, Gold Coast, QLD, Australia

[2]Instituto Nacional de Cardiología, Departamento de Bioquímica, Mexico City, Mexico

Corresponding Author:

Stephen John Ralph, School of Medical Sciences, Griffith University, Parklands Drive, Southport QLD Australia 4222.

Ph: +61 55528583 Fx +61 55528908 email: s.ralph@griffith.edu.au

Word count: 4710, excluding references. 5 Tables, 7 Figures.

Abstract:

Capecitabine induced toxicities such as hand-foot syndrome (HFS) and progression of metastatic cancer are both treatable with concurrent celecoxib as shown in the ADAPT (Activating Cancer Stem Cells from Dormancy And Potentiate for Targeting) trial. In the present study, five commonly used NSAIDs, including celecoxib were compared for their pro-oxidative capacities as cytotoxic drugs against human and mouse metastatic melanoma or breast cancer cells in vitro and the source of cellular ROS production induced by celecoxib was examined in greater detail.

Results: Celecoxib was unique among the NSAIDs in that it showed particular potency as a cytotoxic drug against the metastatic cancer cells with IC_{50} values in the low micromolar range. Celecoxib rapidly enhanced mitochondrial superoxide production *in situ* from cancer cells within minutes, leading to a decrease in cellular respiration and dissipation of the mitochondrial transmembrane potential ($\Delta\psi_m$), followed by extensive ROS-dependent apoptosis of the metastatic cancer cells. Celecoxib also showed rapid and direct effects on isolated mitochondria, inducing extensive ROS production in a dose-dependent manner, whilst it inhibited respiration *via* Complex I or Complex II when tested in whole cells. Mitochondrial ROS production was necessary for the celecoxib induced cell death.

Innovation and Conclusion: These novel findings for direct effects of celecoxib on mitochondria to induce metastatic cancer cell death via a ROS-dependent pro-oxidative mechanism provide supportive evidence for its combinatorial use as a chemosensitizing agent complementing chemotherapies to improve response rates in patients with advanced metastatic cancers.

Abstract: 230 words

Keywords: Metastatic cancer, celecoxib, mechanism of action, mitochondrial ROS, apoptosis

Abbreviations:

$\Delta\psi_m$ mitochondrial transmembrane potential

t-BHP tert-butyl hydroperoxide

COX-2 cyclooxygenase-2

DCFDA 2′,7′-dichlorofluorescein diacetate

DHE dihydroethidium

GI_{50} dose of drug causing 50% inhibition of cell growth by MTT assay

G + M + S glutamate plus malate plus succinate

IC_{50} dose of cytotoxic drug causing 50% cell death by Sytox green dye uptake

Mitocans mitochondria targeted anti-cancer drugs

MnTMPyP Manganese (III) tetrakis(1-methyl-4-pyridyl)porphyrin pentachloride

NSAID non-specific anti-inflammatory drug

OxPhos oxidative phosphorylation

ROS reactive oxygen species

S + R succinate plus rotenone

TMRM tetramethylrhodamine, methyl ester

1. Introduction.

Mitochondria in metastatic cancer cells differ markedly in their metabolism from the majority of primary cancers and normal cells [reviewed in [1, 2]]. Metabolic changes in mitochondria have been established as causing an enhanced pro-oxidative state with increased ROS production leading to cancer cell invasion, migration and metastasis [3-5]. In a dynamic process involving hypoxic stress, cancer cells evolve and progress to greater malignancy with higher ROS levels promoting greater metastasis [6, 7]. However, high ROS levels are generally detrimental to cells, and the redox status of cancer cells differs from that of normal cells, such that cancer cells exhibit elevated ROS, which enables oxidative stress to work as an anticancer strategy [8].

Many cells die from these stressful conditions, but the survivors, undergoing dramatic shifts in redox status with mitochondrial and nuclear damage from ensuing oxidative stress, promote further malignancy and metastasis [6, 9]. This selection pressure, promoted by the combined stressful conditions of hypoxia *plus* hypoglycaemia [10] involves dysfunctional mitochondrial ATP synthesis (*i.e.*, oxidative phosphorylation; OxPhos), causing enhanced release of ROS as a by-product of an impaired respiratory chain, which then causes mutations, particularly in the adjacent susceptible mitochondrial DNA, and eventually enhances metastasis [11-14]. As a consequence, cytosolic Ca^{2+} levels become elevated which helps trigger epithelial-mesenchymal transition, accelerated growth and invasiveness together with the emergence of more highly metastatic cancer stem cells [15]. ROS also stabilize the transcription factor HIF-1α [16] which up-regulates mRNAs encoding several key proteins involved in angiogenesis, cellular proliferation, erythropoiesis, vascularization and glycolysis [17, 18].

These changes to metastatic cancer cells clearly link their greater pro-oxidative states with greater malignancy [6] and present targets for drugs such as NSAIDs to help eliminate cancers [19]. The mitochondrial pro-apoptotic or intrinsic cell death pathway can be activated by promoting increased ROS to reach excessive levels that lead to apoptosis *via* the opening of the mitochondrial membrane permeability transition pore complex [19].

Longitudinal studies of patients using low levels of NSAIDs as analgesics over periods of many years have consistently shown a decrease in cancer incidence by 30%–50% when compared to the non-drug user and general population [20-23], suggesting that NSAIDs may be effective in lowering risk of metastasis [24, 25]. Although the NSAIDs are not commonly considered as anticancer drugs, they can selectively promote the intrinsic pathway of apoptosis in metastatic cancer cells [19] and affect mitochondrial function [26]. Unlike metastatic cancer cells with their highly pro-oxidative state, the normal cells can resist the effects of NSAIDs because they contain higher levels of anti-oxidant defences such as reduced glutathione, catalases, peroxidases, superoxide dismutases, glyoxylases and other ROS reducing enzymes (reviewed in [19]).

In this study, five NSAIDs have been examined for their cytotoxic activity against metastatic breast cancer and melanoma cells. Surprisingly, celecoxib showed the most potent anti-cancer activity among these drugs, affecting mitochondrial function and inducing rapid and significantly higher levels of superoxide production leading to cell death. These pro-oxidative properties and direct effects on mitochondria directly correlated with the cytotoxic activity of the NSAIDs and their ability in the micromolar range to induce extensive metastatic melanoma and breast cancer cell apoptosis. Mitochondrial ROS was shown to be an essential mediator for the activation of apoptosis in metastatic cancer cells.

2. Materials and Methods

2.0. Materials

Reagent	Manufacturer	Country	Lot #	Cat	Solvent
Sytox Green	Life Technologies	USA	1646682		
Annexin-V	BD Pharmingen	AU	3239067		
Acridine Orange	Invitrogen	USA	775222		
MitoSOX	Invitrogen	USA	1802090		
DHE	Sigma Aldrich	USA			
DCF	Sigma Aldrich	USA	075M4092V		
TBHP	Sigma Aldrich	USA	MKCD3314		
MnTMpyP	Abcam	UK	AB142212		
NAc-Cys	Life Technologies	USA	1711803		
a-TOS	Sigma Aldrich	USA	SLBH6145V		
DMC	Sigma Aldrich	USA	SZBD064XV		
Diclofenac	Abcam	UK	AB120621		
Nimesulide	Abcam	UK	AB142926		
Sulindac	Abcam	UK	AB142950		
Salicylate	Abcam	UK	AB120746		
Caspase 3/7 kit	Promega	USA	G8090		
Celecoxib	Sigma Aldrich	USA	LRAA6299	PHR1683	30%DMSO 70%EtOH
	or Pure Chem Scientific	USA	80007427		
2,5-Dimethyl-celecoxib	Sigma Aldrich	USA	113M4603V	D7196	30%DMSO 70%EtOH
Sulindac	Sigma Aldrich	USA	MKCC6957	S4429	Water
Amplex Red	Invitrogen	USA		A12222	DMSO
digitonin	Sigma Aldrich	USA	127K1641	D5628	DMSO
Proteinase, bacterial (Nagarse)	Sigma Aldrich	USA		P8038	Water

2.1. Tissue Culture

All cell lines were sourced from the American Tissue Type Collection (ATCC) and authenticated by MHC or HLA surface markers. Murine melanoma B16F10 cells and 4T1 cells

were maintained in DMEM and RPMI respectively, supplemented with 6% heat-inactivated FBS, 4% heat-inactivated NBCS, Penicillin/Streptomycin, 1.6 mM L-glutamate, supplemented with 1% Glutamax and 20 mM HEPES buffer and incubated at 37°C in a humidified atmosphere of 5% CO_2. Triple negative MDAMB-231 and MDAMB-468 breast, HeLa cervix, MCF-7 breast human cancers and NIH3T3 mouse fibroblast were grown in DMEM (Gibco; Rockville, MD, USA) supplemented with 10% FBS and incubated in 5% CO_2 at 37°C. Cells were harvested via trypsinisation (Gibco) after washing twice with 1 x PBS, and pelleted *via* centrifugation at 1250 rpm for 4 min. Cell counting and viability was determined using trypan blue dye exclusion.

2.2. Drug solubilisation

All drugs used were solubilised as a standard stock of 25 mM. Salicylate and diclofenac were solubilised in d.d. H_2O. Celecoxib, nimesulide and sulindac were solubilised using a 100 mM stock solution of (2-Hydroxypropyl)-β-cyclodextrin (Sigma-Aldrich). Solubilisation of celecoxib was also performed in DMSO 30%/ethanol 70%. Turbidity analysis at λ = 500 and 600 nm, revealed no crystal formation in 10 mM stock solutions. The maximal amount of vehicle DMSO/ethanol used (20-30 μL) was assayed in respiration, $\Delta\psi m$ and cellular proliferation experiments alone compared to control with no apparent effect by vehicle.

2.3. Determining cytotoxic IC_{50} values

Initially, the in vitro screening of the five NSAIDs tested for their cytotoxic activity against cancer cells was examined over a range of concentrations from 0 to 1 mM. The aim was to find those with potency in the low micromolar range, providing the rationale for further examining their off target activity on mitochondria, given previous findings with NSAIDs [26] and our preliminary evaluation of the literature reviewed in [19]. For each NSAID tested on the

cell lines, the cytotoxic IC_{50} values were determined using 96-well black wall, flat bottomed plates (Corning). Cell death was determined (A) with the use of Sytox green (Thermofisher Scientific) at a final concentration of 500 nM to differentiate viable from non-viable cell populations. Plates were read on a Flexstation 3 (Molecular Devices) spectrophotometer every 24 h for a total of 72 h; and (B) by using the MTT assay. IC_{50} values were based on the drug concentration causing 50% reduction based on 100% live control *vs.* 100% dead (0.1% triton-x-100 treated) cell populations as determined by Sytox green (Thermo Fisher Scientific) dye exclusion (approximate fluorescence excitation/emission maxima: 504/523 nm, bound to DNA) and GI_{50} values were defined as the drug concentration causing 50% growth inhibition of the treated cells compared to vehicle treated cell population standardised as 100% by plotting dose-response curves over time in days of cell culture. Celecoxib (0.1-1000 μM) was added at the beginning of the cell cultures and the GI_{50} was determined at the 24 or 72 h-time point. The data shown represent the mean ± S.D. of at least 3-4 different assayed preparations. Statistical analysis was made using the standard Student's t-test.

2.4. Apoptosis

Apoptosis was determined using the FITC-Annexin V Apoptosis Detection Kit (BD Biosciences) following the manufacturer's protocol. Cells were seeded into 6-well plates at a density of 2 x 10^5 cells *per* well and incubated for 24 h before adding NSAIDs at the appropriate concentration and incubated for the indicated amount of time. Stained cells were then placed on ice and analysed using a BD Fortessa flow cytometer. Acridine Orange staining was performed in triplicate after incubating cells for 3 h in 100 μM celecoxib and stained for 15 min at 2 μg/mL before imaging on an Olympus IX53 microscope. Shift in fluorescence signals from

excitation/emission maxima of 502/525nm to 460/650nm in the lysosomes was examined. For caspase 3/7 activation the Caspase-Glo 3/7 reagent from Promega was used following the manufacturer's protocol after incubation with celecoxib (at 100 μM to ensure significant activation of caspase occurred) and for the times as indicated.

2.5. Mitochondrial transmembrane potential ($\Delta\Psi_m$) in isolated cancer cells

Mitochondrial transmembrane potential ($\Delta\Psi_m$) was assayed by staining cells with rhodamine 6G (0.25 μM) before monitoring changes in fluorescence of whole cancer cells treated over the responsive range of celecoxib concentrations (0-20 μM) compared to untreated control cells (set as 100%). The changes in $\Delta\Psi_m$ were monitored with a Shimadzu spectrofluorophotometer (RF-5301PC; Tokyo, Japan) at 480 nm (excitation) and 565 nm (emission) wavelengths. The maximal change in magnitude of the fluorescence signal for $\Delta\Psi_m$ was determined by comparing $\Delta\Psi_m$ before and after dissipation with the protonophore CCCP (5 μM) at the end of each experiment (Hernández-Reséndiz et al., 2015).

2.6. Determining mitochondrial and cytosolic ROS production

Mitochondrial superoxide was measured using the MitoSOX^{TM}red kit (Life Technologies) and staining following the manufacture's protocol. Cells were seeded at 2 x 10^5 in 6-well plates and incubated for 48 h. Cells were treated with drug and incubated for a further 2-6 h. Samples were harvested, stored at 4°C before analysis with the BD LSRFortessa™ cell analyser (BD Biosciences). For MitoSOXred, dihydroethidium (DHE) or DCFDA measurements in 96-well black wall plates, 10^5 cells/mL were seeded and incubated for 48 h before staining and drug addition (as indicated) before reading on a FlexStation 3 Multi-Mode Microplate Reader

(Molecular Devices). For timed responses, cell suspensions (10^6/mL) were prepared, stained for 10 min at 37°C, with periodic gentle vortexing and then stored at 4°C before analysis. Immediately prior to analysis, cell samples were warmed to 37°C in a water bath for 60 s and baseline readings obtained before adding drug and continuously reading every 6 min.

The rate of H_2O_2 production was also assessed by using Amplex Red (Invitrogen) in the presence of an excess of peroxidase [27]. AS-30 D isolated mitochondria (0.2-0.45 mg protein/mL) were incubated at 37°C in the KME-Pi buffer with 4-5 μM Amplex Red and 5 U/mL horse radish peroxidase (Sigma); the absorbance difference at 573 *minus* 595 nm was determined using a dual-beam spectrophotometer (2501PC, Shimadzu, Japan).

2.7. Mitochondria isolation from rat AS-30D hepatoma, heart and liver tissue.

For AS-30D mitochondria isolation, the digitonin permeabilization procedure was performed as previously described [28, 29]. The final mitochondrial pellet was washed with SHE (Sucrose 250 mM, HEPES 10 mM, EGTA 1 mM pH 7.4) buffer and incubated with 0.5% (w/v) fatty acid free-albumin and 1 mM ADP for 15 min at 4°C before final centrifugation.

Rat liver [30] or heart [31] mitochondria were isolated using the sequential centrifugation method as described previously. For rat heart mitochondria isolation, Nagarse (Sigma Chem.) was used at 6 mg *per* 4 hearts for a digestion time of 8 min on ice. The mitochondrial pellet was resuspended in SHE buffer at 50-80 mg protein/mL.

2.8. Oxygen consumption and OxPhos flux in isolated mitochondria and cells

For isolated mitochondria, respiration of AS-30D, heart and liver mitochondria (0.5-1 mg protein/mL) was assayed using an oxygraph with a Clark-type O_2 electrode in KME (120 mM

KCl, 20 mM Mops, 1 mM EGTA) buffer pH 7.2 with 2 mM KH_2PO_4, and in the presence of different oxidizable substrates (as indicated in Results section) at 37°C. Drugs were added to the medium before mitochondrial addition. Mitochondrial state 3 respiration was stimulated with 600 nmol ADP.

For OxPhos, cells were incubated in Krebs-Ringer (125 mM NaCl, 5 mM KCl, 25 mM HEPES, 1.4 mM $CaCl_2$, 1mM KH_2PO_4, 1mM $MgCl_2$, pH7.4) buffer in the presence of glucose (5 mM) at 37°C. Drugs were added to the medium before cell addition. OxPhos flux was determined by measuring the oligomycin (5 µM) sensitive respiration with a Clark-type O_2 electrode as previously described [32].

2.9. Microscopy

All fluorescence and light field microscopy was performed using an Olympus IX50 microscope and cellSens software (Olympus). For fluorescent imaging, exposure times and minima/maxima light fields were set to a standard level based on the signals from untreated and negative *vs.* positive controls. For MitoSOXred imaging, cells were plated at a density of 10^5 cells/mL in sterile 96 well black wall culture plates for 48h before incubating with NSAID for 60 min. Confocal images were performed using a Leica SP-8 confocal microscope after seeding 4 x 10^4 cells on an 8-well u-Slide (Ibidi) overnight, and staining with MitoSOXred and nuclear counterstaining with Hoescht 33342 for 10 min before celecoxib addition.

2.10. Statistics

Experiments determining cytotoxic IC_{50} values were repeated twice by two independent researchers. Each experiment was conducted with a minimum of 3 replicates. For determining apoptosis, mitochondrial transmembrane potential, mitochondrial and cytosolic ROS levels, each

experiment was repeated at least twice with a minimum of three replicates each time to determine mean values ± Standard Deviation (SD) unless otherwise indicated. N.D. = not determined. Statistical analysis was performed using Graphpad Prism (version 6.1) and Microcal Origin (version 8E) software and statistical significance was determined using ANOVA or standard Student's t-test.

3. Results

3.1. Celecoxib is a potent cytotoxic drug for metastatic melanoma and breast cancer cells, inducing extensive death by the mitochondrial apoptosis signalling pathway.

A number of the NSAIDs are pro-drugs with critical Cys-thiol reactivity as one possible modality for activating the mitochondrial permeability pore and thereby inducing apoptosis of metastatic cancer cells [19]. However, the specific actions of NSAIDs on mitochondrial function and mechanisms for activating the intrinsic pathway of apoptosis in metastatic cancer cells have not yet been fully established. In an initial study, five NSAIDs, including the third generation cyclooxygenase-2 (COX-2) selective celecoxib, were compared for dose- and time-dependent cytotoxic activity against two murine metastatic cell lines, B16F10 melanoma and 4T1 breast cancer (IC_{50}; Table 1A), as well as their growth inhibitory effects on several other metastatic, non-metastatic and non-cancerous cell lines (GI_{50}; Fig. 1A, Table 1B).

When compared to untreated cells across a concentration range 0- 200 μM, celecoxib was clearly the most potent growth inhibitor of the five different NSAIDs (Fig. 1A). Celecoxib also induced complete cell death in both B16F10 and 4T1 cells after 72 h at 100 μM concentration, with a dose-dependent increase in Sytox green signal detected as early as 24 h (Fig. 2A).

Celecoxib significantly diminished cell growth at 25 μM when given as a single dose over 72 h, whereas the other NSAIDs were much less potent as cytotoxic anticancer drugs (Table 1A & B).

Cell growth assays were carried out comparing the GI_{50} values for the NSAIDs, including celecoxib and its COX-2 independent derivative, dimethyl-celecoxib [33, 34] using a range of cell lines. At 24 h, celecoxib and dimethyl-celecoxib showed the highest levels of growth inhibitory activity against the two human metastatic breast cancer cell lines (MDA-MB-231 and MDA-MB-468; GI_{50} = 6-27 μM) compared to other less sensitive cell lines (HeLa or MCF-7; GI_{50} = 71-90 μM) (Table 1B). Over the 24 to 72 h period, the GI_{50} of celecoxib for the non-malignant cells (normal 3T3 murine fibroblasts) was also higher (69-90 μM).

Next, B16F10 and 4T1 cells were exposed to each NSAID using its IC_{50}/72 h concentration and apoptosis levels assayed after 24 h (Fig. 1C). All of the NSAIDs increased the levels of apoptosis over the control (with the exception of salicylate that was assayed at the maximum concentration of 800 μM). On the basis of the above results, the five NSAIDs were then compared when applied using a fixed concentration of 50 μM for 48 h (Fig. 1D). Again, celecoxib proved the most potent, causing extensive apoptosis by 48 h in both B16F10 and 4T1 cell lines (mean 63% and 67% apoptosis respectively).

To further assess for apoptosis, whole B16F10 and 4T1 cells were assayed and nuclear blebbing imaged using Sytox green as one indicator of apoptosis, as well as by using Acridine Orange staining to identify lysosomal formation, indicative of autophagy events. The concentration of celecoxib used (100 μM) was above the IC50 to ensure rapid activation of enhanced levels of apoptosis. Thus, apoptotic B16F10 cells with nuclear blebbing were detected by 24 h after treatment with 100 μM celecoxib (Fig. 2A). Even as early as 3 h after treatment

with 100 μM celecoxib, Acridine Orange staining showed lysosomal formation indicative of autophagy, together with Sytox green nuclear blebbing and chromatin condensation indicating apoptosis (Fig. 2B & C). To confirm that celecoxib was inducing apoptosis *via* the mitochondrial signalling pathway, B16F10 cells were assayed for caspase 3/7 activity which increased significantly by 2-fold within 4 h of treatment with 100 μM celecoxib (Fig. 2D). By 18 h of treatment with 100 μM of celecoxib, the level of caspase 3/7 activity had returned to that of the untreated controls, consistent with later stages of apoptosis. Hence, celecoxib rapidly induced mitochondrial mediated apoptosis, associated with increased signs of autophagy.

3.2. Selected NSAIDs rapidly induce significant increases in ROS production detected as mitochondrial superoxide in metastatic cancer cells.

To further investigate the mechanisms for the NSAID-mediated toxicity on the metastatic B16F10 and 4T1 cancer cells, the ability of the NSAIDs to promote cellular ROS production was analysed. Exposing these two cell lines to 50 μM of each NSAID did not significantly change the endogenous levels of cytosolic ROS detected by DCFDA in the B16F10 cell line over 2 to 24 h of treatment (Fig. 3A), with the exception of a significant salicylate-induced increase detected at 24h. Slightly increased cytosolic ROS was obtained with 50 μM *tert*-butyl hydroperoxide (TBHP) added as a positive control for producing ROS inside the cells. Hence, the present data indicate that cytosolic levels of ROS were not greatly affected by the NSAIDs.

Next, ROS production at the mitochondrial level was analysed using the fluorescent indicator dye MitoSOX^{TM}red to detect mitochondrial superoxide [35]. Table 2A summarises the data for each of the NSAIDs, tested at different concentrations (as indicated) reflecting their IC_{50} values for their abilities over the first hour after adding drug to promote mitochondrial ROS

production. Of the NSAIDs, celecoxib was markedly more active at inducing significantly increased mitochondrial ROS production, even with low concentrations of added drug. These results were confirmed both by spectrophotometry (Fig. 3B) and fluorescence microscopy with celecoxib tested for 1 h over the range of 50-200 μM (Fig. 3; Panel D). Of the five NSAIDs, only celecoxib displayed such a markedly increased mitochondrial ROS signal above that of the control or vehicle alone treated cells.

Next, B16F10 cells were exposed to each individual NSAID fixed at 50 μM and the superoxide production levels assayed at regular 2 h intervals for up to 6 h. Alpha-tocopherol succinate (α-TOS), a known potent inducer of mitochondrial superoxide [36], was included as a positive control for enhancing mitochondrial ROS production (Table 2A). Celecoxib was the only NSAID that induced greater levels of mitochondrial superoxide production by 2 h (39% increase over control; Fig 3C). However, by 4 h, the celecoxib treated B16F10 cells showed substantially greater mitochondrial superoxide (137% increase above control cells; Fig. 3C), with diclofenac then displaying a non-significant increase. By 6 h, all five of the NSAID-treated B16F10 samples started to show increased mitochondrial superoxide production, with both diclofenac and nimesulide induced levels then becoming significant (Fig. 3C, 103% and 118% increase respectively). By 6 h, the celecoxib induced levels of ROS production started decreasing, consistent with a transient oxidative burst of mitochondrial superoxide taking place.

To examine the NSAID induced mitochondrial superoxide production more closely, treated cell samples were assayed by flow cytometry at regular 6 min intervals for up to 84 min (Fig. 4A). Celecoxib induced significant mitochondrial superoxide production in both the B16F10 and 4T1 metastatic cells, detected as early as 12 min after drug addition, becoming strongly significant in both cell lines by 84 min, when compared to untreated controls.

Nimesulide was the only other NSAID that increased the levels of mitochondrial superoxide production over this time course, and only in the B16F10 cells (Fig. 4A). These findings indicated that celecoxib at this concentration (50 μM) was able to rapidly induce mitochondrial superoxide production over short time periods, whereas the other NSAIDs have a more delayed mechanism of action, or are active only at much higher concentrations.

3.3. Pre-treating cells with the superoxide dismutase mimetic, MnTMPyP, significantly inhibits the formation of mitochondrial superoxide induced by celecoxib in both B16F10 and 4T1 cells

To ensure that the superoxide signal observed with MitoSOXred was emanating from the mitochondria, high resolution confocal microscopy was performed after treatment with 100 μM celecoxib for 1 h. Image panels in Figure 4C demonstrate greatly increased mitochondrial superoxide production detected as higher MitoSOXred signal as compared to untreated controls (Figure 4B). Moreover, nuclear DNA staining by dihydroethidium (DHE), which is produced after mitochondrial reaction of MitoSOXred with superoxide [37], showed that as early as 1 h, translocation of DHE into the cell nuclei was visibly present (counterstained using DAPI; Fig. 4D).

To identify whether the superoxide ROS signal obtained from celecoxib could be blocked and thereby prevent drug-induced apoptosis, both the B16F10 and 4T1 cell lines were pre-treated with the potent mitochondrial superoxide dismutase (SOD) mimetic, MnTMPyP [38] as a mitochondrial targeted antioxidant before addition of celecoxib for a further 2 to 4 h. Tert-butyl hydroperoxide (TBHP) alone treated cells were used as a positive control for ROS production. MnTMPyP pre-treating cells before adding celecoxib inhibited the superoxide

production levels in both cell lines, causing significant loss of the MitoSOXred signal at both the 2 and 4 h time points (Fig. 5A & B). Furthermore, DHE staining in the cell nuclei was completely absent when cells were first pre-treated for 10 min with MnTMPyP before 2 h of celecoxib treatment (image panel; Fig. 5C). Also, comparing the untreated versus celecoxib treated cells either with or without MnTMPyP pre-treatment, again showed a marked absence of nuclear DHE staining visible when the potent SOD mimetic was present (Fig. 5D image panel).

The pro-oxidative drug, α-TOS, was examined as a positive control for ROS as we had previously established that this drug promoted mitochondrial ROS production required to activate cancer cell apoptosis [36]. In line with our previous report, pre-treating B16F10 cells with MnTMPyP [50 μM] for 1 h inhibited the superoxide signal induced by α-TOS at 3 h (Fig. 6A, B). Furthermore, pre-treating the B16F10 cells with MnTMPyP [50 μM] for 1 h also partially reversed the celecoxib [50 μM] induced level of cell death at 48h from 40 to 20%, indicating that the mitochondrial ROS signal induced by celecoxib was required to activate cell death (Fig. 6B). These findings confirm a requirement for the celecoxib-induced mitochondrial ROS in triggering subsequent cancer cell apoptosis.

3.4. Celecoxib inhibits respiration and $\Delta\psi_m$ of human tumor cells

To examine the sensitivity of mitochondria in human metastatic cancer cell lines to celecoxib, the triple negative metastatic breast cancer lines MDA-MB231 and MDA-MB468 were used and the effects of up to 200 μM drug assayed on the respiratory rates (Table 2B) and $\Delta\psi_m$ (Table 2C) in cultured whole cells. The results showed that the mitochondrial respiratory function in these metastatic human breast cancer cell lines was highly sensitive to the effects of this NSAID, even at the low μM range, consistent with the celecoxib concentrations required to

inhibit the growth of these cells (Table 1B). Next, the effect of celecoxib on tetramethylrhodamine, methyl ester (TMRM) uptake was analysed as a cell-permeant, cationic, red-orange fluorescent dye that is readily sequestered by active mitochondria as an indicator of the levels of mitochondrial transmembrane potential ($\Delta\psi_m$). Celecoxib addition also caused a decrease in $\Delta\psi_m$ in a dose-dependent manner over the 5 to 20 μM range (Fig. 7A), associated with inhibition of respiration, consistent with the severe decrease detected in cell proliferation (Table 1B). The IC_{50} values determined for the celecoxib mediated inhibition of $\Delta\psi_m$ were low, at 6-6.7 μM for both of the MDA-MB231 and MDA-MB468 cell lines (Fig. 7A). Celecoxib over similar concentrations inhibited OxPhos (*i.e.*, oligomycin-sensitive respiration) (Table 2B) and decreased $\Delta\psi_m$ in the human metastatic breast cancer cell lines, as well as in the cervical adenocarcinoma HeLa cells (Table 2C). Dimethylcelecoxib, the non-COX-2 analogue showed similar inhibitory effects on OxPhos and $\Delta\psi_m$ of the triple negative breast cancer cell lines (Tables 2B and 2C).

3.5. Celecoxib directly induces ROS production from isolated mitochondria and inhibits the respiratory rates in cancer cells.

The preceding results suggested that celecoxib could be directly affecting metastatic cell mitochondria, promoting their levels of ROS production. To further explore this possibility, purified mitochondria were isolated from fresh rat heart and liver or from AS-30D rat hepatocarcinoma ascites fluid as a ready source [29] and assayed for the direct effects of celecoxib on the mitochondrial respiratory rates and associated levels of ROS production. Celecoxib treatment of isolated rat liver mitochondria showed a dose-dependent inhibition of respiratory rates from State 3 and State 4 control values, particularly noticeable at higher

concentrations of celecoxib (250 to 500 μM) and in short-term experiments of 2-5 min (Table 3). Celecoxib inhibition was greater when mitochondria were respiring on glutamate + malate (G+M) with higher celecoxib concentrations (250 and 500 μM) causing 70-90% inhibition (Table 3). The respiratory control ratios (state 3 rate/state 4 rate) were also significantly decreased by ~50% at 100 μM celecoxib, across the different substrate conditions (Table 3), consistent with an ensuing inhibition of $\Delta\psi_m$ derived from proton leak/uncoupling and then respiratory chain inhibition occurring with successively higher amounts of added drug (Table 2C).

Increasing concentrations of celecoxib (0-500 μM) decreased the rat liver mitochondrial state 3 respiratory rate independently of the substrate used. Extending the treatment time by pre-incubating with drug (0-500 μM celecoxib, Table 4) for 15 min before measuring respiration rates did not show a greater inhibitory effect. Celecoxib was also highly active on heart mitochondria, particularly noticeable when succinate was included as substrate (either as G+M+S, or S + R). When succinate + rotenone (S+R) was used as substrate, celecoxib (250-500 μM) inhibited respiration by 70-80%. This result suggested a possible preference in heart mitochondria for inhibiting succinate driven Complex II function when celecoxib is at this higher concentration. In addition, the inhibitory effect of celecoxib at 250 μM on rat heart mitochondria State 3 respiration was not as marked when G + M (50 % inhibition; n=4) were used as substrates compared to succinate alone (S + R, 70-80%; Table 3). Heart mitochondrial State 4 respiration was unaltered even when higher celecoxib doses were applied. These data suggest that when mitochondria are isolated and removed from the context of normal cells, such that the cytosolic antioxidant defences are taken away, the mitochondria then become sensitive to the direct actions of celecoxib on respiration.

For mitochondria isolated from AS-30D hepatoma cells (Table 4), celecoxib did not significantly change the State 3 and 4 respiration rates, showing a slight decrease in State 3 at 50, 250 and 500 μM, with all substrates assayed. These results further indicated that ***isolated*** normal mitochondria are more susceptible to the effects of celecoxib than are the ***isolated*** tumor mitochondria. This difference in celecoxib sensitivity between mitochondria types (normal *versus* tumor) could be related to the higher content of cholesterol (20-times) found in the tumor mitochondrial membranes compared to rat liver mitochondria [39]. Cholesterol makes membranes more rigid which may interfere with drug transport and uptake into the mitochondrial matrix [40].

Next, the effect of celecoxib on the level of ROS production from isolated AS-30D hepatocarcinoma cells as a ready source of tumor cell mitochondria were assayed using the sensitive Amplex red dye [41]. A rapid and significant dose-dependent increase in ROS production from the isolated mitochondria was immediately detected after celecoxib addition, increasing over the concentration range tested (up to 50 μM), compared to the negligible levels of ROS produced by untreated AS-30D mitochondria respiring on either G + M or S (Fig. 7B). This increased ROS correlated well with the effects of celecoxib on the mitochondrial superoxide production observed in whole metastatic cancer cells over a similar concentration range (Fig. 4A). Effects of celecoxib on ROS production were also observed with isolated liver and heart mitochondria respiring on G+M or S (data not shown). The latter data with Amplex Red confirms the results using MitoSOXred to detect ROS produced by mitochondria in whole cells (Fig. 3, Fig. 4) and together these findings are the first demonstration that celecoxib has rapid and direct effects on isolated mitochondrial ROS production, possibly mediated by modifying the activity of the respiratory complexes CI and/or CII.

4. Discussion

4.1. NSAID cytotoxicity on cancer cells

Given the frequently observed decreased incidence of cancer from longitudinal studies of patients using low doses of NSAIDs for analgesic purposes (Wang et al., 2015, Guadagni et al., 2007, Friis et al., 2015, Algra and Rothwell, 2012) including preventing metastasis [25], much interest has arisen concerning the use of NSAIDs as potential anticancer therapies. In fact, recent results from a Phase II study have exemplified the clinical potential of celecoxib as a drug which greatly enhances survival and complete responses in patients with advanced Stage IV metastatic colorectal cancers when celecoxib was used as a treatment in combination with the chemotherapy, Capecitabine [42].

The five NSAIDs examined showed marked variation in their IC_{50} values, although with the exception of salicylate, the other NSAIDs either decreased cell growth and/or increased cell death in a dose- and time-dependent fashion. Celecoxib was by far the most potent NSAID for inducing cell death in the range of metastatic cell lines tested here, including against human triple negative breast cancer cells, where it was active even at the low micromolar concentration. Diclofenac also induced cell death, although it required four-fold higher concentrations than celecoxib. Nimesulide restricted cell growth when at concentrations above 100 μM, but was not a significant inducer of cell death compared to either celecoxib or diclofenac. Both sulindac and salicylate only induced cell death at very high μM to low mM concentrations making these unlikely to be achievable or useful as a therapy *in vivo*.

In the present study, celecoxib showed marked activity against the human triple negative breast cancer cell lines, decreasing proliferation within 24 h when using low levels (GI_{50} at 24h

was ~6 μM for MDA-MB468; and ~20 μM for MDA-MB231). In these studies, the metastatic cancer cells were only exposed to a single dose of drug added at the start of the assays, with monitoring over periods of 24-72 h. Repeated daily doses of low (1-10 μM) celecoxib levels administered to the metastatic cancer cells could sustain much higher accumulative drug actions and effects *in vitro*, with a greater net cytotoxic activity and further decrease IC_{50} and GI_{50} values in a system more closely mimicking an *in vivo* dosing regimen [43]. In this regard, low and physiologically relevant levels (1-10 μM) of celecoxib have been reported to chemosensitize cancer cells to subsequent treatment with common cytotoxic chemotherapeutic drugs such as doxorubicin [44, 45] and greatly enhances chemotherapeutic anti-metastatic cancer cell efficacy *in vitro* and *in vivo* [44, 46], as well as in clinical trials of metastatic colorectal cancer patients [42].

4.2. Celecoxib induces mitochondrial ROS production required for triggering cancer cell death by apoptosis.

Our novel findings reported here clearly highlight previously unrecognised effects of the NSAIDs such as celecoxib on mitochondrial respiration and function. The data presented here establish that celecoxib is a potent anticancer agent which can directly and rapidly affect mitochondrial O_2 uptake by causing excessive mitochondrial superoxide production. This pro-oxidative activity of celecoxib is essentially required for the triggering of extensive cell death via the intrinsic apoptotic pathway because its action is prevented by pre-treating cells with the potent anti-oxidative SOD mimetic, MnTMPyP. These findings of excessive mitochondrial ROS production explain the previously reported celecoxib mediated mechanism of action inside cancer cells shown to proceed via the mitochondrial apoptosis signalling pathway [47]. Results from other studies are entirely consistent with our own findings presented here that celecoxib is

cytotoxic for cancer cells independent of its effects on COX-2 [48, 49], particularly for the closely related, COX-2 non-inhibitory analogue, dimethylcelecoxib, which shows even greater anticancer activity [50-52]. Our results establish that celecoxib increases mitochondrial ROS levels to trigger the ensuing cytotoxic actions of the drug, activating the intrinsic apoptotic pathway in metastatic cancer cells by disrupting mitochondrial metabolism and induces excessive ROS production directly from the mitochondria as an essential part of this death signalling process.

4.3. Celecoxib promotes mitochondrial ROS production at levels below those inhibiting respiratory function.

This is the first report demonstrating the mechanism for the direct actions of celecoxib on mitochondria, either isolated or inside cells, showing in both situations that the drug induces rapid ROS production at lower doses of drug (5-50 μM) than those required to inhibit respiratory rates (>100 μM), when either Complex I or II substrates are available for use. In addition, the ability of celecoxib to inhibit respiration was greater for State 3 respiration (*i.e.*, oxidative phosphorylation) under conditions where succinate was present. Interactions of celecoxib with the respiratory chain complexes involving either the FAD or a ubisemiquinone intermediate could be sources for the ROS production proceeding *via* electron leakage from the complexes interacting with molecular O_2 to form superoxide [53].

Celecoxib at concentrations of less than 50 μM was clearly superior to other NSAIDs tested for their anti-metastatic cancer cell cytotoxicity and this activity correlated well with ROS production levels. The ability of celecoxib to inhibit the $\Delta\psi_m$ would also suggest that inhibiting the respiratory chain function, in a manner similar to that of the Complex III inhibitor Antimycin

A [54] facilitates collapse of the mitochondrial transmembrane potential in the metastatic cancer cells. The combined effects of ROS and loss of $\Delta\psi_m$ most likely contribute to inducing the ensuing intrinsic apoptosis pathway in celecoxib treated metastatic cancer cells.

4.4. Clinical relevance of celecoxib anti-cancer activity to drug pharmacokinetics in humans.

We have included a table of recommended NSAID dosage per day, resulting peak serum concentrations, calculated maximum available concentrations (μM values) and source references (Table 5), particularly relating to celecoxib in humans. Based on this data, levels of celecoxib can be achieved in the 10 to 20 μM range which are sufficient and capable of effectively killing cancer cells *in vivo*. Analysis of peak plasma concentrations for celecoxib from patients taking daily doses (400mg) for rheumatoid arthritis (RA) and (800mg, as a 400mg does taken twice-daily) for familial adenomatous polyposis (FAP) after 3-4 hours reached ~4 μM and ~8 μM respectively [55]. Peak levels depend on patient CYP2A9 versus CYP2C8 polymorphisms of the cytochrome P450 oxidases which metabolise celecoxib [56]. Interestingly, patients given 200-mg celecoxib + 200-mg ketoconazole daily for 7 days to inhibit CYP enzymes showed the highest Cmax 12 μM, with no side effects [55]. More recent advances in drug delivery based around mixtures of polyvinylpyrolidone (PVP)/ d-α-Tocopheryl polyethylene glycol 1000 succinate (TPGS) as solid dispersion nanoparticles [57] or supersaturating self-emulsifying drug delivery systems (S-SEDDS) [58] have significantly increased the dissolution and orally administered bioavailability of celecoxib. The area under the concentration-time curve (AUC 0→24 h) and peak plasma concentration (Cmax) was increased several fold using celecoxib-PVP-TPGS formulations [57] or S-SEDDS with the highest Cmax reaching 8 μg/ml (or 20 μM) in rat plasma after 3-4 hours [58, 59]. The human equivalent dose (HED) based on the FDA

guidelines for body area would be 16 mg/kg or 800mg/day for a 50 kg person. Recently, a liquid formulation of celecoxib (aka DFN-15) was developed which gave improved median time to peak concentration (Tmax) within 1 h whereas 2.5 h was required for the oral capsules [60]. The pharmacokinetics of DFN-15 was dose proportional over the range tested (120 to 240 mg) and the Cmax after administering DFN-15 at 120, 180, and 240 mg (1062–1933 ng/ml; 2.7 - 5 μM) were much higher than for the 400mg oral capsules (611 ng/ml) [60]. However, 400mg oral capsules provided higher sustained levels over 72 hours with AUC (8 μg h/ml). Given the IC_{50} for celecoxib obtained in the present study of 25-30 μM after 96 hours, reaching the range of physiologically relevant plasma concentrations should be achievable and tolerable over one to two weeks of treatment. In addition, considering that the present study was based on the use of only a single dose with monitoring over 72-96 hours, it is probable that a treatment regime using repeated daily dosing over several days of up to 800 mg would bring the concentration of celecoxib to within the 10-20 μM range, in line with clinically relevant values. Furthermore, with celecoxib demonstrating a significant killing of both cell lines at ~ 10 μM from a single dose, then such a repeated daily dosing scheme (400mg capsule twice-daily) should provide levels sufficient for killing *in vivo*. In this regard, it should be noted that many studies have reported use of celecoxib doses at these levels as an adjunct therapy in combination with common chemotherapeutic drugs (such as doxorubicin or 5-flurouracil). Several trials have demonstrated synergism with either a marked decrease in the levels of chemotherapy required to be effective or enhanced anticancer efficacy when given as combination therapy for advanced stage metastatic cancers [44, 61-66].

Mitochondrial targeted anticancer drugs (Mitocans) can be considered as promising to help eradicate chemotherapy resistant cancer cells because they directly promote pro-oxidative

stress to affect mitochondria independent of upstream signalling events and offer new perspectives for developing innovative and more effective combinatorial cancer therapies [1]. The COX-2 independent effects of celecoxib are shown here as directly inducing increased mitochondrial ROS production to enhance death of metastatic cancer cells. This finding provides the supportive mechanistic evidence justifying using celecoxib as an approved pharmaceutical either as a standalone or in combination treatment for the eradication of metastatic lesions, as has been shown previously *in vivo* or in clinical trials now in many studies [44, 67-71], and as summarized in Fig. 3G. The duality of such treatments should result in better patient outcomes and remission rates [42], but also help to reduce the toxicities of chemotherapy and may decrease the relative amounts of drugs that are required**.**

Author Contributions: S.J.R. and R.P. devised, planned and designed the study with input from R.M-S. and S.R. S.J.R., R.M-S. and S.R. acquired funding to support the work, analysed and interpreted the data. R.P. acquired, analysed and interpreted the murine cell data for Fig. 1-5, with input from V.B. R.M-S, S.C. P-V. and S.R. contributed the data from human cells and isolated mitochondrial respiration in Fig 6 and Tables 1-4. R.P. and S.J.R. compiled the draft manuscript and figures, with other authors contributing to the final revising of the manuscript and approving submission.

Acknowledgements: Funding - The present work was partially supported by CONACyT-Mexico grants No. 239930 and 281428 to RMS. Rhys Pritchard was supported by an Australian postgraduate research award (APRA).

Author Disclosure Statement: The authors have no conflicts of interest and no competing financial interests exist.

Tables

Table 1. NSAID cytotoxicity (IC_{50}) and growth inhibition (GI_{50}) values

A. NSAID IC_{50} / [µM] at 72 h

Cell Line	NSAID
	Celecoxib
B16F10	57 ± 12
4T1	49 ± 4
	Diclofenac
B16F10	261 ± 12
4T1	227 ± 28
	Nimesulide
B16F10	461 ± 50
4T1	393 ± 37
	Sulindac
B16F10	>800
4T1	558 ± 58
	Salicylate
B16F10	>800
4T1	>800

B. NSAID GI_{50} / [µM] at 24 - 72 h

Cell Line	24 h	72 h
	Celecoxib	
HeLa	71 ± 28	43 ± 15
MDA MB-231	27 ± 11	34 ± 10
MDA MB-468	6 ± 1	20.5 ± 2
MCF-7	90 ± 6	69 ± 11
3T3	92 ± 28	69 ± 7
	Dimethyl celecoxib	
HeLa	59 ± 12	43 ± 18
MDA MB-231	71 ± 9	116 ± 18
MDA MB-468	115 ± 18	81 ± 9
MCF-7	62 ± 4	87 ± 23
3T3	94 ± 33	53 ± 9
	Sulindac	
HeLa	N.D.	99 ± 29
MDA MB-231	212 ± 87	395 ± 36
MDA MB-468	270 ± 131	675 ± 113
MCF-7	>1000	>1000
3T3	>1000	498 ± 89

Table 2. Effects of NSAIDs on mitochondrial superoxide, cellular OXPHOS and $\Delta\Psi_m$

A. Mitochondrial ROS (MitoSOXred)*

Drug/ Cell Line	Concentration [μM]		
αTOS/	**100**	**200**	**400**
B16F10	3.6 ± 0.7	4.8 ± 1.4	4.5 ± 0.8
4T1	6 ± 2.3	6.3 ± 2.9	6.1 ± 1.6
Celecoxib/	**25**	**50**	**100**
B16F10	1.2 ± 0.2	2.7 ± 0.5	4.7 ± 1.2
4T1	1.4 ± 0.1	2.8 ± 0.1	13.8 ± 0.9
Diclofenac/	**100**	**200**	**400**
B16F10	1.2 ± 0.2	1.3 ± 0.3	1.5 ± 0.4
4T1	1.7 ± 0.3	1.5 ± 0.3	1.5 ± 0.2
Nimesulide/	**100**	**200**	**400**
B16F10	1.3 ± 0.3	1.9 ± 0.3	3.9 ± 1.1
4T1	1.1 ± 0.1	1.3 ± 0.1	6.6 ± 1.9
Sulindac/	**200**	**400**	**800**
B16F10	1.7 ± 0.1	3.6 ± 1.0	1.8 ± 0.6
4T1	1.5 ± 0.7	4.7 ± 3.1	4.9 ± 0.9
Salicylate/	**200**	**400**	**800**
B16F10	0.6 ± 0.1	0.4 ± 0.1	0.5 ± 0.1
4T1	1.2 ± 0.1	1.4 ± 0.2	1.5 ± 0.4

* Ratio relative to control values (no added drug)

B. OXPHOS (ngAtO/min/mg protein)

DRUG/ [μM]	CELECOXIB		DIMETHYL CELECOXIB	
	MDA MB-231	**MDA MB-468**	**MDA MB-231**	**MDA MB-468**
0	18.5 ± 7	23 ± 14	12.5 ± 4	7.5 ± 4
20	15 ± 5	23 ± 11	10 ± 4	4 ± 2
50	11 ± 7	20 ± 17	7 ± 4	2 ± 2
100	5 ± 3	10 ± 5	5 ± 2	1.7 ± 1.7
200	3 ± 1	6 ± 3	2 ± 2	1 ± 0.8
	HELA	**MCF-7**	**HELA**	**MCF-7**
0	15 ± 6	21 ± 5	12 ± 2	20 ± 5
20	5 ± 0.3	18 ± 2.5	10.5 ± 4	19 ± 8.5
50	3.5 ± 3	14 ± 3	2 ± 0.6	15 ± 12
100	3 ± 0.5	6 ± 4	2 ± 0.6	14 ± 14
200	2 ± 2	3 ± 3	4 ± 0.8	9 ± 9

C. $\Delta\Psi_m$ (FAU)

DRUG/ [μM]	CELECOXIB		DIMETHYL CELECOXIB	
	MDA MB-231	**MDA MB-468**	**MDA MB-231**	**MDA MB-468**
0	209 ± 125	179 ± 105	155 ± 27	165 ± 17
5	122 ± 110	120 ± 67	100 ± 40	151 ± 15
10	47 ± 40	49 ± 47	48 ± 23	88 ± 39
20	28 ± 22	33 (n=2)	0 ± 0	3 ± 5
	HELA	**MCF-7**	**HELA**	**MCF-7**
0	162 ± 34	127 ± 75	145 ± 10	133 ± 25
5	109 ± 22	86 ± 46	72 ± 21	76 ± 29
10	74 ± 16	49 ± 2	30 ± 8	43 ± 27
20	80 ± 5	5 ± 9	7 ± 6	4 ± 1.5

FAU: Fluorescence Arbitrary Units ± SD

Table 3. Celecoxib effects on substrate oxidation of isolated rat liver or heart mitochondria.

RAT LIVER MITOCHONDRIA (RLM)						RAT HEART MITOCHONDRIA (RHM)					
Sub-strates	**Cele-coxib**	**Pst 4**	**St 3**	**St4**	**RC**	**Sub-strates**	**Cele-coxib**	**Pst 4**	**St 3**	**St4**	**RC**
G+M	**[µM]**	**ngAtO/min/mg protein**				**G+M**	**[µM]**	**ngAtO/min/mg protein**			
	0	34 ± 10	150 ± 47	18 ± 0.1	7.4 ± 2		**0**	88 ± 31	555 ± 244	138 ± 83	4.7 ± 1.8
	50	63 ± 18	175 ± 42	48 ± 8	5.8 ± 3		**50**	91 ± 37	470 ± 197	145 ± 50	3.4 ± 1.3
	100	106 ± 50	90 ± 36	21 ± 18	5.2 ± 4		**100**	114 ± 53	426 ± 179	154 ± 56	2.9 ± 1.0
	250	7 ± 2	7 ± 3	6 ± 2	4 ± 3		**250**	85 ± 50	303 ± 150	77 ± 51	2.6 ± 1.8
	500	5 (n=2)	5 (n=2)	5 (n=2)	1 (n=2)		**500**	62 ± 26	116 ± 70	76 ± 65	2.4 ± 1.9
G+M+S	**0**	55 ± 22	167 ± 37	24 ± 9	7 ± 3	**G+M+S**	**0**	79 ± 25	480 ± 55	143 ± 85	4.1 ± 2.6
	50	68 ± 33	216 ± 102	54 ± 35	4 ± 2		**50**	109 ± 53	413 ± 123	161 ± 87	2.9 ± 1.2
	100	41 ± 7	82 ± 65	63 ± 52	2.1 ± 1.9		**100**	118 ± 59	320 ± 23	129 ± 76	3.4 ± 2.3
	250	50 ± 11	107 ± 69	24 ± 5	3.4 ± 2.4		**250**	105 ± 85	304 ± 22	51 ± 11	2.8 ± 3.1
	500	55 ± 23	108 ± 104	12 ± 9	2.4 ± 1.5		**500**	79 ± 27	93 ± 49	93 ± 49	1 ± 1.0
S+R	**0**	71 ± 45	208 ± 84	63 ± 50	4.3 ± 2	**S+R**	**0**	85 ± 37	425 ± 140	221 ± 40	3.4 ± 1.8
	50	86 ± 48	191 ± 66	90 ± 70	3.3 ± 2.3		**50**	90 ± 37	386 ± 109	151 ± 72	2.6 ± 0.9
	100	74 ± 44	181 ± 90	88 ± 59	1.5 ± 0.9		**100**	126 ± 56	395 ± 96	114 ± 12	3.2 ± 2.5
	250	48 ± 34	100 ± 63	16 ± 7	1 ± 0.8		**250**	46 ± 18	166 ± 95	59 ± 17	1.7 ± 1.3
	500	25 (n=2)	9 (n=2)	9 (n=2)	1 ± 1.0		**500**	81 ± 24	83 ± 54	91 ± 54	1 ± 1.0

Abbreviations: G, glutamate 5mM; M, malate 5 mM; S, succinate 0.5 mM; R, rotenone 2 µM. Pst 4, pseudo-state 4 (respiratory rate before adding ADP); St 3, state 3 respiration (ADP-stimulated respiratory rate); St 4, state 4 respiration (ADP-exhausted respiratory rate); RC (respiratory control, St3/St4 ratio). Values represent mean of 3-5 ± S.D of independent preparations, unless otherwise identified. *p<0.001; **p<0.01 vs. control.

Table 4. Celecoxib and substrate oxidation of RLM or mitochondria from AS-30D ascites.

RAT LIVER MITOCHONDRIA/ CELECOXIB 15 MIN PRE-INCUBATION ⊥						AS-30D ASCITES MITOCHONDRIA					
Sub-strates	**Cele -coxib**	**Pst 4**	**St 3**	**St4**	**RC**	**Sub-strates**	**Cele-coxib**	**Pst 4**	**St 3**	**St4**	
G+M	**[µM]**	**ngAtO/min/mg protein**				**G+M**	**[µM]**	**ngAtO/min/mg protein**			**RC**
	0	52	125	26	5.3		**0**	40 ± 14	168 ± 22	50 ± 4	3.4 ± 0.5
	50	44	78	24	3.4		**50**	39 ± 8	150 ± 47	53 ± 10	2.8 ± 0.4
	100	42	105	26	4.6		**100**	51 ± 8	181 ± 24	75 ± 8	2.4 ± 0.5
	250	69	76	32	2.6		**250**	30 ± 22	190 (2)	54 ± 43	1.9 ± 0.8
	500	87	87	91	1.6		**500**	39 ± 30	183 (2)	59 (2)	1.1 ± 0.2
G+M+S	**0**	67	98	35	3.1	**G+M+S**	**0**	62 ± 13	192 ± 29	70 ± 19	2.9 ± 1.1
	50	51	103	24	1.8		**50**	62 ± 4	196 ± 28	88.5 ± 20	2.3 ± 0.8
	100	71	127	48	1.4		**100**	71.5 ± 35	183 ± 33	88.5 ± 25	2.2 ± 0.8
	250	89	121	40	2.2		**250**	57.5 ± 6	190 (2)	79 ± 25	1.7 ± 0.8
	500	54	145	18	8.0		**500**	54 ± 20	117 ± 77	108 ± 75	1.1 ± 0.1
S+R	**0**	100	172	69	2.4	**S+R**	**0**	77 ± 30	202 ± 63	68 ± 35	3.0 ± 1.0
	50	85	152	71	2.3		**50**	71 ± 22	197 (2)	74 ± 41	1.9 ± 1.3
	100	98	160	98	1.7		**100**	82 ± 29.5	164 ± 66	76 ± 35	2.3 ± 0.9
	250	107	148	74	1.9		**250**	49.5 ± 32	168 (2)	58 ± 34	1.7 ± 0.9
	500	145	236	100	2.3		**500**	58 ± 46	177 (2)	43 (2)	1.1 ± 0.2

⊥Preincubation with celecoxib at 37°C in KME buffer and after 15 min, respiration rates were determined. Abbreviations: G, glutamate 5mM; M,malate 5 mM for RLM or malate 0.1 mM for AS-30D; S, succinate 0.5 mM; R, rotenone 2 µM. Pst 4, pseudo-state 4 (respiratory rate before adding ADP); St 3, state 3 respiration (ADP-stimulated respiratory rate); St 4, state 4 respiration (ADP-exhausted respiratory rate); RC (respiratory control, St3/St4 ratio). Values show the mean of 2 for RLM pre-incubated with drug. AS-30D mitochondria were measured directly upon addition of drug and show mean ± S.D. of 3-4 independent preparations, unless otherwise indicated (mean of (2)).

Table 5: NSAID dose recommended per day, maximum individual dosages, peak serum concentrations, calculated maximum available μM values and source references.

NSAID	MW (g/Mol)	Max/Day (mg)	Max/Dose (mg)	$T_{1/2}$ (Hours)	Cmax* (μg/ml)	Cmax (μM)	Tmax (Hours)	REF
Celecoxib	381.4	400-800 (400mg BiD)	200-400	11.2	1.5-2.9 (1.8)	7.6	1.6-4.6	[55-60, 72]
Diclofenac	318.1	150	50-75	2.5-5.9	2.367	7.44	2 (1-4)	[73]
Nimesulide	308.3	200	100	3.24	2.860	9.28	1.2-2.8	[74, 75]
Sulindac	356.4	400	200	7.8	4.700	14.03	1.6	[76-78]
Salicylate	160.1	3600-5400	1000	2.4-19	180	529.01	0.75	[79-83]

*Cmax (μM) values are calculated based on the maximum allowable single dosage and peak plasma (Cmax; μg/mL) corresponding to that dosage.

#Mean average values have been used and a range provided where available.

Figure legends

Figure 1. Analysis of five different NSAIDs for their cytotoxicity levels on metastatic B16F10 melanoma and 4T1 breast cancer lines.

A) B16F10 and 4T1 72 h cell growth assay with NSAID treatment over a concentration range up to 200 μM. **B)** Marked increase in Sytox green dye uptake after 24 h (I) vehicle treated control, (II) 150 μM celecoxib. Magnification bar represents 100μm **C)** % Apoptotic B16F10 or 4T1 cells induced by each of the NSAIDs treated using the 72 h IC_{50} concentration and analysed after 24 h. Heat treated (60°C/10 min) and TBHP treated (200 μM) were used as positive controls for apoptosis. **D)** Apoptosis induced by treating B16F10 or 4T1 for 48 h with a standardized concentration (50 μM) of NSAID. * indicates significant difference compared to control ($p<0.05$).

Figure 2. Apoptotic nuclei, lysosome formation and caspase 3/7 activity post treatment with Celecoxib

A) B16F10 cell nuclei vehicle treated (I) or 100 μM celecoxib treated (II) for 24 h, stained using Sytox green with characteristic nuclear fragmentation indicative of apoptosis. **B)** B16F10 cells after 3 h either untreated (I) or celecoxib (100 μM) treated (II), demonstrating low pH lysosomal formation by Acridine Orange staining as well as nuclear blebbing, again confirming apoptotic induction and auto/mitophagy. **C)** 4T1 cells treated under conditions as for B) with Acridine Orange staining, showing untreated cells (III) versus celecoxib (100 μM) treated, (IV). Scale is 10 μM. **D)** Caspase 3/7 activity measured 4 h and 18 h in the B16F10 cell line after addition of celecoxib (100 μM) with αTOS (200 μM) as a positive control. Significance (*) is to $p < 0.05$.

Figure 3. Mitochondrial superoxide produced after treatment with NSAIDs

A) Each NSAID (50 μM) assayed for cytosolic ROS detected using DCF after 2 h or 24 h treatment. Terbutyl hydroperoxide (TBHP, 50 μM for 2 h) and N-acetylcysteine (NAC, 5 mM for 1 h) were used as positive and negative controls respectively. **B)** Change in superoxide levels detected by DHE after treating cells for 1 h with increasing concentrations of celecoxib for B16F10 and 4T1 cells. **C)** Change in MitoSOX red signals at 2, 4 and 6 h upon exposing B16F10 cells to each NSAID (50 μM) assayed via FACS with αTOS (50 μM) used as a positive ROS control. **D)** Image panel, untreated 4T1 cells (I) vehicle treated cells (II) αTOS (200 μM) treated (III) and celecoxib (100 μM) treated (IV) cells after 1 h stained with MitoSOX red and imaged using fluorescence microscopy. Bottom row (V) diclofenac, (VI) nimesulide, (VII) sulindac and (VIII) salicylate all at 200 μM for 1 h (Note that no other NSAID assayed at these concentrations (50-200 μM) and time point (1 h) displayed a detectable increase in mitochondrial superoxide in either cell line compared to control). Scale bar represents 100 microns. Significance (*) is to $p < 0.05$.

Figure 4. Early detection of MitoSOX signal in whole cells and confocal imaging

A) Changes in MitoSOX red signals assayed at 6 min intervals when treating B16F10 or 4T1 cells respectively with each NSAID (50 μM) analysed by flow cytometry. **B and C)** Confocal micrographs of B16F10 cells untreated (**B**, I-III) or treated (**C**, I-III) with celecoxib (100 μM) for 1 h. Scale bar represents 30 microns. G) Magnified images of celecoxib treated B16F10 cells (100 μM) with Hoescht 33342 (I), MitoSOXred (II) or combined superimposed (III) images. Cell

nuclei were counter stained with Hoescht 33342 for 10 min and images obtained with a Leica SP-8 confocal microscope. Scale represents 30 microns.

Figure 5. Celecoxib induced superoxide production in whole cells is abrogated by pre-treating with MnTMPyP.

A and B) MnTMPyP [10 μM] pre-treatment for 10 min significantly abrogates the celecoxib (50 μM) induced superoxide production in both B16F10 and 4T1 cells at 2 h and 4 h. TBHP (200 μM) was used as a positive control for ROS induction, as determined with DHE staining and spectrofluorometry. **C)** Inhibition of nuclear DHE staining by pre-treating cells with MnTMPyP: (I) B16F10 cells treated with 200 μM TBHP for 2 h (II) B16F10 cells pre-incubated with 10 μM MnTMPyP for 10 min prior to adding 200 μM TBHP for 2 h. Images obtained by fluorescence microscopy, with scale bar 100 microns. **D)** Decreased DHE nuclear fluorescence signal assessed by microscopy after pre-treating cells with 10 μM MnTMPyP for 10 min: (I) untreated 4T1 cells; (II) untreated 4T1 cells with MnTMPyP (10 μM); (III) celecoxib treated (50 μM); and (IV) celecoxib treated (50 μM) with MnTMPyP (10 μM) after two hours. Scale represents 30 microns. Significance (*) is to $p < 0.05$.

Figure 6. Pre-treating cells with MnTMPyP inhibits ROS induced by alpha-TOS and partially reverses celecoxib induced cell death.

A. Right side panel: 50 μM MnTMPyP (Mn) pre-treatment for 1 h before addition of alpha-TOS (αTS) [200 μM] significantly abrogates the superoxide signal detected as DHE nuclear staining in B16F10 cells detected at 3 h. Left side panel: Representative fluorescence micrograph of DHE

nuclear staining in B16F10 cells. I: untreated cells, II: Mn/vehicle alone treated cells, III: Alpha-TOS alone treated, IV: Mn pre-treated + alpha-TOS. Scale bar 30 microns.

B. Percent live B16F10 cells after 48h treatment with Mn/vehicle alone or pre-treated with Mn for 1 h before addition of celecoxib at the concentration shown compared to untreated control cells.

Figure 7. Celecoxib induces ROS directly from isolated mitochondria as well as inhibiting $\Delta\Psi_m$ in whole tumor cells.

A) Mitochondrial transmembrane potential ($\Delta\Psi_m$) was assayed by monitoring changes in rhodamine 6G fluorescence in whole cancer cells treated over a range of celecoxib concentrations compared to untreated control cells (set as 100%, for absolute values see **Table 2C**). **B**) Celecoxib induced ROS production from isolated hepatoma mitochondria. Drug at concentrations as indicated was added directly to isolated AS-30D mitochondria whilst measuring basal ROS production by changes in absorbance of Amplex Red. Arrow indicates point of addition of celecoxib at concentrations indicated. **C**) Model for application of celecoxib as a chemosensitizing agent by inducing mitochondrial superoxide production (ROS) if combined with current commonly used chemo/radiotherapy based treatments to promote enhanced cancer cell death.

References

[1] S.J. Ralph, P. Low, L. Dong, A. Lawen, J. Neuzil, Mitocans: mitochondrial targeted anti-cancer drugs as improved therapies and related patent documents, Recent Pat Anticancer Drug Discov 1(3) (2006) 327-46.
[2] E.I. Chen, Mitochondrial dysfunction and cancer metastasis, J Bioenerg Biomembr 44(6) (2012) 619-22.
[3] A. Hall, K.D. Meyle, M.K. Lange, M. Klima, M. Sanderhoff, C. Dahl, C. Abildgaard, K. Thorup, S.M. Moghimi, P.B. Jensen, J. Bartek, P. Guldberg, C. Christensen, Dysfunctional oxidative phosphorylation makes malignant melanoma cells addicted to glycolysis driven by the (V600E)BRAF oncogene, Oncotarget 4(4) (2013) 584-99.
[4] P.E. Porporato, P. Sonveaux, Paving the way for therapeutic prevention of tumor metastasis with agents targeting mitochondrial superoxide, Mol Cell Oncol 2(3) (2015) e968043.
[5] P.E. Porporato, V.L. Payen, J. Perez-Escuredo, C.J. De Saedeleer, P. Danhier, T. Copetti, S. Dhup, M. Tardy, T. Vazeille, C. Bouzin, O. Feron, C. Michiels, B. Gallez, P. Sonveaux, A mitochondrial switch promotes tumor metastasis, Cell Rep 8(3) (2014) 754-66.
[6] S.J. Ralph, S. Rodriguez-Enriquez, J. Neuzil, E. Saavedra, R. Moreno-Sanchez, The causes of cancer revisited: "mitochondrial malignancy" and ROS-induced oncogenic transformation - why mitochondria are targets for cancer therapy, Mol Aspects Med 31(2) (2010) 145-70.
[7] R.C. Ji, Hypoxia and lymphangiogenesis in tumor microenvironment and metastasis, Cancer Lett 346(1) (2014) 6-16.
[8] C. Gorrini, I.S. Harris, T.W. Mak, Modulation of oxidative stress as an anticancer strategy, Nat Rev Drug Discov 12(12) (2013) 931-47.
[9] S.S. Sabharwal, P.T. Schumacker, Mitochondrial ROS in cancer: initiators, amplifiers or an Achilles' heel?, Nat Rev Cancer 14(11) (2014) 709-21.
[10] A. Marin-Hernandez, J.C. Gallardo-Perez, I. Hernandez-Resendiz, I. Del Mazo-Monsalvo, D.X. Robledo-Cadena, R. Moreno-Sanchez, S. Rodriguez-Enriquez, Hypoglycemia Enhances Epithelial-Mesenchymal Transition and Invasiveness, and Restrains the Warburg Phenotype, in Hypoxic HeLa Cell Cultures and Microspheroids, J Cell Physiol (2016).
[11] K. Ishikawa, K. Takenaga, M. Akimoto, N. Koshikawa, A. Yamaguchi, H. Imanishi, K. Nakada, Y. Honma, J. Hayashi, ROS-generating mitochondrial DNA mutations can regulate tumor cell metastasis, Science 320(5876) (2008) 661-4.
[12] K. Ishikawa, J. Hayashi, A novel function of mtDNA: its involvement in metastasis, Ann N Y Acad Sci 1201 (2010) 40-3.
[13] K. Ishikawa, H. Imanishi, K. Takenaga, J. Hayashi, Regulation of metastasis; mitochondrial DNA mutations have appeared on stage, J Bioenerg Biomembr 44(6) (2012) 639-44.
[14] J.B. Nunes, J. Peixoto, P. Soares, V. Maximo, S. Carvalho, S.S. Pinho, A.F. Vieira, J. Paredes, A.C. Rego, I.L. Ferreira, M. Gomez-Lazaro, M. Sobrinho-Simoes, K.K. Singh, J. Lima, OXPHOS dysfunction regulates integrin-beta1 modifications and enhances cell motility and migration, Hum Mol Genet 24(7) (2015) 1977-90.
[15] M. Guha, S. Srinivasan, G. Ruthel, A.K. Kashina, R.P. Carstens, A. Mendoza, C. Khanna, T. Van Winkle, N.G. Avadhani, Mitochondrial retrograde signaling induces epithelial-mesenchymal transition and generates breast cancer stem cells, Oncogene 33(45) (2014) 5238-50.
[16] S.N. Jung, W.K. Yang, J. Kim, H.S. Kim, E.J. Kim, H. Yun, H. Park, S.S. Kim, W. Choe, I. Kang, J. Ha, Reactive oxygen species stabilize hypoxia-inducible factor-1 alpha protein and

stimulate transcriptional activity via AMP-activated protein kinase in DU145 human prostate cancer cells, Carcinogenesis 29(4) (2008) 713-21.
[17] A. Weidemann, R.S. Johnson, Biology of HIF-1alpha, Cell Death Differ 15(4) (2008) 621-7.
[18] A. Marin-Hernandez, J.C. Gallardo-Perez, S.J. Ralph, S. Rodriguez-Enriquez, R. Moreno-Sanchez, HIF-1alpha modulates energy metabolism in cancer cells by inducing over-expression of specific glycolytic isoforms, Mini Rev Med Chem 9(9) (2009) 1084-101.
[19] S.J. Ralph, R. Pritchard, S. Rodriguez-Enriquez, R. Moreno-Sanchez, R.K. Ralph, Hitting the Bull's-Eye in Metastatic Cancers-NSAIDs Elevate ROS in Mitochondria, Inducing Malignant Cell Death, Pharmaceuticals (Basel) 8(1) (2015) 62-106.
[20] X. Wang, U. Peters, J.D. Potter, E. White, Association of Nonsteroidal Anti-Inflammatory Drugs with Colorectal Cancer by Subgroups in the VITamins and Lifestyle (VITAL) Study, Cancer Epidemiol Biomarkers Prev 24(4) (2015) 727-35.
[21] F. Guadagni, P. Ferroni, R. Palmirotta, G. Del Monte, V. Formica, M. Roselli, Non-steroidal anti-inflammatory drugs in cancer prevention and therapy, Anticancer Res 27(5A) (2007) 3147-62.
[22] S. Friis, A.H. Riis, R. Erichsen, J.A. Baron, H.T. Sorensen, Low-Dose Aspirin or Nonsteroidal Anti-inflammatory Drug Use and Colorectal Cancer Risk: A Population-Based, Case-Control Study, Ann Intern Med 163(5) (2015) 347-55.
[23] A.M. Algra, P.M. Rothwell, Effects of regular aspirin on long-term cancer incidence and metastasis: a systematic comparison of evidence from observational studies versus randomised trials, Lancet Oncol 13(5) (2012) 518-27.
[24] P.M. Rothwell, M. Wilson, J.F. Price, J.F. Belch, T.W. Meade, Z. Mehta, Effect of daily aspirin on risk of cancer metastasis: a study of incident cancers during randomised controlled trials, Lancet 379(9826) (2012) 1591-601.
[25] X. Zhao, Z. Xu, H. Li, NSAIDs Use and Reduced Metastasis in Cancer Patients: results from a meta-analysis, Sci Rep 7(1) (2017) 1875.
[26] R. Moreno-Sanchez, C. Bravo, C. Vasquez, G. Ayala, L.H. Silveira, M. Martinez-Lavin, Inhibition and uncoupling of oxidative phosphorylation by nonsteroidal anti-inflammatory drugs: study in mitochondria, submitochondrial particles, cells, and whole heart, Biochem Pharmacol 57(7) (1999) 743-52.
[27] R. Moreno-Sanchez, L. Hernandez-Esquivel, N.A. Rivero-Segura, A. Marin-Hernandez, J. Neuzil, S.J. Ralph, S. Rodriguez-Enriquez, Reactive oxygen species are generated by the respiratory complex II--evidence for lack of contribution of the reverse electron flow in complex I, FEBS J 280(3) (2013) 927-38.
[28] R.W. Moreadith, G. Fiskum, Isolation of mitochondria from ascites tumor cells permeabilized with digitonin, Anal Biochem 137(2) (1984) 360-7.
[29] S. Rodriguez-Enriquez, O. Juarez, J.S. Rodriguez-Zavala, R. Moreno-Sanchez, Multisite control of the Crabtree effect in ascites hepatoma cells, Eur J Biochem 268(8) (2001) 2512-9.
[30] R. Moreno-Sanchez, Regulation of oxidative phosphorylation in mitochondria by external free Ca2+ concentrations, J Biol Chem 260(7) (1985) 4028-34.
[31] R. Moreno-Sanchez, R.G. Hansford, Dependence of cardiac mitochondrial pyruvate dehydrogenase activity on intramitochondrial free Ca2+ concentration, Biochem J 256(2) (1988) 403-12.
[32] I. Hernandez-Resendiz, A. Roman-Rosales, E. Garcia-Villa, A. Lopez-Macay, E. Pineda, E. Saavedra, J.C. Gallardo-Perez, E. Alvarez-Rios, P. Gariglio, R. Moreno-Sanchez, S. Rodriguez-

Enriquez, Dual regulation of energy metabolism by p53 in human cervix and breast cancer cells, Biochim Biophys Acta 1853(12) (2015) 3266-78.
[33] L.M. Backhus, N.A. Petasis, J. Uddin, A.H. Schonthal, R.D. Bart, Y. Lin, V.A. Starnes, R.M. Bremner, Dimethyl celecoxib as a novel non-cyclooxygenase 2 therapy in the treatment of non-small cell lung cancer, J Thorac Cardiovasc Surg 130(5) (2005) 1406-12.
[34] A. Kardosh, W. Wang, J. Uddin, N.A. Petasis, F.M. Hofman, T.C. Chen, A.H. Schonthal, Dimethyl-celecoxib (DMC), a derivative of celecoxib that lacks cyclooxygenase-2-inhibitory function, potently mimics the anti-tumor effects of celecoxib on Burkitt's lymphoma in vitro and in vivo, Cancer Biol Ther 4(5) (2005) 571-82.
[35] K.M. Robinson, M.S. Janes, J.S. Beckman, The selective detection of mitochondrial superoxide by live cell imaging, Nat Protoc 3(6) (2008) 941-7.
[36] L.F. Dong, P. Low, J.C. Dyason, X.F. Wang, L. Prochazka, P.K. Witting, R. Freeman, E. Swettenham, K. Valis, J. Liu, R. Zobalova, J. Turanek, D.R. Spitz, F.E. Domann, I.E. Scheffler, S.J. Ralph, J. Neuzil, Alpha-tocopheryl succinate induces apoptosis by targeting ubiquinone-binding sites in mitochondrial respiratory complex II, Oncogene 27(31) (2008) 4324-35.
[37] H. Zhao, S. Kalivendi, H. Zhang, J. Joseph, K. Nithipatikom, J. Vasquez-Vivar, B. Kalyanaraman, Superoxide reacts with hydroethidine but forms a fluorescent product that is distinctly different from ethidium: potential implications in intracellular fluorescence detection of superoxide, Free Radic Biol Med 34(11) (2003) 1359-68.
[38] C. Moriscot, S. Candel, V. Sauret, J. Kerr-Conte, M.J. Richard, M.C. Favrot, P.Y. Benhamou, MnTMPyP, a metalloporphyrin-based superoxide dismutase/catalase mimetic, protects INS-1 cells and human pancreatic islets from an in vitro oxidative challenge, Diabetes Metab 33(1) (2007) 44-53.
[39] S. Rodriguez-Enriquez, L. Hernandez-Esquivel, A. Marin-Hernandez, M. El Hafidi, J.C. Gallardo-Perez, I. Hernandez-Resendiz, J.S. Rodriguez-Zavala, S.C. Pacheco-Velazquez, R. Moreno-Sanchez, Mitochondrial free fatty acid beta-oxidation supports oxidative phosphorylation and proliferation in cancer cells, Int J Biochem Cell Biol 65 (2015) 209-21.
[40] L. Zhang, W.F. Bennett, T. Zheng, P.K. Ouyang, X. Ouyang, X. Qiu, A. Luo, M. Karttunen, P. Chen, Effect of Cholesterol on Cellular Uptake of Cancer Drugs Pirarubicin and Ellipticine, J Phys Chem B 120(12) (2016) 3148-56.
[41] M. Zhou, Z. Diwu, N. Panchuk-Voloshina, R.P. Haugland, A stable nonfluorescent derivative of resorufin for the fluorometric determination of trace hydrogen peroxide: applications in detecting the activity of phagocyte NADPH oxidase and other oxidases, Anal Biochem 253(2) (1997) 162-8.
[42] E.H. Lin, S.A. Patel, J. Chou, E.Y. Kim, V. Shankaran, A.L. Coveler, W.P. Harris, J.O. Park, A. Fichera, G.N. Mann, E.G. Chiorean, C.C. Pritchard, M. Sinanan, M. Upton, B. Storer, R.S. Yeung, L. Li, A phase II trial of maintenance ADAPT therapy targeting colon cancer stem cells in patients with metastatic colorectal cancer, Journal of Clinical Oncology 32(15_suppl) (2014) TPS3650-TPS3650.
[43] C.S. Williams, A.J. Watson, H. Sheng, R. Helou, J. Shao, R.N. DuBois, Celecoxib prevents tumor growth in vivo without toxicity to normal gut: lack of correlation between in vitro and in vivo models, Cancer Res 60(21) (2000) 6045-51.
[44] J. van Wijngaarden, E. van Beek, G. van Rossum, C. van der Bent, K. Hoekman, G. van der Pluijm, M.A. van der Pol, H.J. Broxterman, V.W. van Hinsbergh, C.W. Lowik, Celecoxib enhances doxorubicin-induced cytotoxicity in MDA-MB231 cells by NF-kappaB-mediated increase of intracellular doxorubicin accumulation, Eur J Cancer 43(2) (2007) 433-42.

[45] C. Chen, W. Xu, C.M. Wang, Combination of celecoxib and doxorubicin increases growth inhibition and apoptosis in acute myeloid leukemia cells, Leuk Lymphoma 54(11) (2013) 2517-22.
[46] S. Hashitani, M. Urade, N. Nishimura, T. Maeda, K. Takaoka, K. Noguchi, K. Sakurai, Apoptosis induction and enhancement of cytotoxicity of anticancer drugs by celecoxib, a selective cyclooxygenase-2 inhibitor, in human head and neck carcinoma cell lines, Int J Oncol 23(3) (2003) 665-72.
[47] V. Jendrossek, R. Handrick, C. Belka, Celecoxib activates a novel mitochondrial apoptosis signaling pathway, FASEB J 17(11) (2003) 1547-9.
[48] M.I. Patel, K. Subbaramaiah, B. Du, M. Chang, P. Yang, R.A. Newman, C. Cordon-Cardo, H.T. Thaler, A.J. Dannenberg, Celecoxib inhibits prostate cancer growth: evidence of a cyclooxygenase-2-independent mechanism, Clin Cancer Res 11(5) (2005) 1999-2007.
[49] B. Xu, Y. Wang, J. Yang, Z. Zhang, Y. Zhang, H. Du, Celecoxib induces apoptosis but up-regulates VEGF via endoplasmic reticulum stress in human colorectal cancer in vitro and in vivo, Cancer Chemother Pharmacol 77(4) (2016) 797-806.
[50] C. Sobolewski, J. Rhim, N. Legrand, F. Muller, C. Cerella, F. Mack, S. Chateauvieux, J.G. Kim, A.Y. Yoon, K.W. Kim, M. Dicato, M. Diederich, 2,5-Dimethyl-celecoxib inhibits cell cycle progression and induces apoptosis in human leukemia cells, J Pharmacol Exp Ther 355(2) (2015) 308-28.
[51] A.H. Schonthal, Antitumor properties of dimethyl-celecoxib, a derivative of celecoxib that does not inhibit cyclooxygenase-2: implications for glioma therapy, Neurosurg Focus 20(4) (2006) E21.
[52] P. Pyrko, A. Kardosh, Y.T. Liu, N. Soriano, W. Xiong, R.H. Chow, J. Uddin, N.A. Petasis, A.K. Mircheff, R.A. Farley, S.G. Louie, T.C. Chen, A.H. Schonthal, Calcium-activated endoplasmic reticulum stress as a major component of tumor cell death induced by 2,5-dimethyl-celecoxib, a non-coxib analogue of celecoxib, Mol Cancer Ther 6(4) (2007) 1262-75.
[53] C.L. Quinlan, I.V. Perevoschikova, R.L. Goncalves, M. Hey-Mogensen, M.D. Brand, The determination and analysis of site-specific rates of mitochondrial reactive oxygen species production, Methods Enzymol 526 (2013) 189-217.
[54] M. Kalbacova, M. Vrbacky, Z. Drahota, Z. Melkova, Comparison of the effect of mitochondrial inhibitors on mitochondrial membrane potential in two different cell lines using flow cytometry and spectrofluorometry, Cytometry A 52(2) (2003) 110-6.
[55] N.M. Davies, A.J. McLachlan, R.O. Day, K.M. Williams, Clinical pharmacokinetics and pharmacodynamics of celecoxib: a selective cyclo-oxygenase-2 inhibitor, Clin Pharmacokinet 38(3) (2000) 225-42.
[56] R. Prieto-Perez, D. Ochoa, T. Cabaleiro, M. Roman, S.D. Sanchez-Rojas, M. Talegon, F. Abad-Santos, Evaluation of the relationship between polymorphisms in CYP2C8 and CYP2C9 and the pharmacokinetics of celecoxib, J Clin Pharmacol 53(12) (2013) 1261-7.
[57] E.S. Ha, G.H. Choo, I.H. Baek, M.S. Kim, Formulation, characterization, and in vivo evaluation of celecoxib-PVP solid dispersion nanoparticles using supercritical antisolvent process, Molecules 19(12) (2014) 20325-39.
[58] W.H. Song, D.W. Yeom, D.H. Lee, K.M. Lee, H.J. Yoo, B.R. Chae, S.H. Song, Y.W. Choi, In situ intestinal permeability and in vivo oral bioavailability of celecoxib in supersaturating self-emulsifying drug delivery system, Arch Pharm Res 37(5) (2014) 626-35.
[59] A.L. Laine, D. Price, J. Davis, D. Roberts, R. Hudson, K. Back, P. Bungay, N. Flanagan, Enhanced oral delivery of celecoxib via the development of a supersaturable amorphous

formulation utilising mesoporous silica and co-loaded HPMCAS, Int J Pharm 512(1) (2016) 118-125.
[60] A. Pal, S. Shenoy, A. Gautam, S. Munjal, J. Niu, M. Gopalakrishnan, J. Gobburru, Pharmacokinetics of DFN-15, a Novel Oral Solution of Celecoxib, Versus Celecoxib 400-mg Capsules: A Randomized Crossover Study in Fasting Healthy Volunteers, Clin Drug Investig 37(10) (2017) 937-946.
[61] L.C. Hou, F. Huang, H.B. Xu, Does celecoxib improve the efficacy of chemotherapy for advanced non-small cell lung cancer?, Br J Clin Pharmacol 81(1) (2016) 23-32.
[62] A.R. Bassiouny, A. Zaky, H.M. Neenaa, Synergistic effect of celecoxib on 5-fluorouracil-induced apoptosis in hepatocellular carcinoma patients, Ann Hepatol 9(4) (2010) 410-8.
[63] E.H. Lin, E.Y. Kim, L. Wang, C. Fong, V. Shankaran, X. Wu, ADAPT therapy vs capecitabine bevacizumab in stage IV colorectal cancer: Pooled 10-year survival experience and a phase II study update., J Clin Oncol 34(15_suppl) (2017).
[64] S. Zhao, J. Cai, H. Bian, L. Gui, F. Zhao, Synergistic inhibition effect of tumor growth by using celecoxib in combination with oxaliplatin, Cancer Invest 27(6) (2009) 636-40.
[65] E.P. Araujo-Mino, Y.Z. Patt, C. Murray-Krezan, J.A. Hanson, P. Bansal, B.J. Liem, A. Rajput, M.H. Fekrazad, G. Heywood, F.C. Lee, Phase II Trial Using a Combination of Oxaliplatin, Capecitabine, and Celecoxib with Concurrent Radiation for Newly Diagnosed Resectable Rectal Cancer, Oncologist 23(1) (2018) 2-e5.
[66] T. Irie, M. Tsujii, S. Tsuji, T. Yoshio, S. Ishii, S. Shinzaki, S. Egawa, Y. Kakiuchi, T. Nishida, M. Yasumaru, H. Iijima, H. Murata, T. Takehara, S. Kawano, N. Hayashi, Synergistic antitumor effects of celecoxib with 5-fluorouracil depend on IFN-gamma, Int J Cancer 121(4) (2007) 878-83.
[67] E.M. Connolly, J.H. Harmey, T. O'Grady, D. Foley, G. Roche-Nagle, E. Kay, D.J. Bouchier-Hayes, Cyclo-oxygenase inhibition reduces tumour growth and metastasis in an orthotopic model of breast cancer, Br J Cancer 87(2) (2002) 231-7.
[68] N. Kundu, A.M. Fulton, Selective cyclooxygenase (COX)-1 or COX-2 inhibitors control metastatic disease in a murine model of breast cancer, Cancer Res 62(8) (2002) 2343-6.
[69] G. Roche-Nagle, E.M. Connolly, M. Eng, D.J. Bouchier-Hayes, J.H. Harmey, Antimetastatic activity of a cyclooxygenase-2 inhibitor, Br J Cancer 91(2) (2004) 359-65.
[70] C. Chen, H.L. Shen, J. Yang, Q.Y. Chen, W.L. Xu, Preventing chemoresistance of human breast cancer cell line, MCF-7 with celecoxib, J Cancer Res Clin Oncol 137(1) (2011) 9-17.
[71] S.H. Kim, S.H. Kim, Y.C. Song, Y.S. Song, Celecoxib potentiates the anticancer effect of cisplatin on vulvar cancer cells independently of cyclooxygenase, Ann N Y Acad Sci 1171 (2009) 635-41.
[72] D. Stempak, J. Gammon, J. Klein, G. Koren, S. Baruchel, Single-dose and steady-state pharmacokinetics of celecoxib in children, Clin Pharmacol Ther 72(5) (2002) 490-7.
[73] M. Mustofa, S. Suryawati, I. Dwiprahasto, B. Santoso, The relative bioavailability of diclofenac with respect to time of administration, Br J Clin Pharmacol 32(2) (1991) 246-7.
[74] A. Bernareggi, The pharmacokinetic profile of nimesulide in healthy volunteers, Drugs 46 Suppl 1 (1993) 64-72.
[75] A. Bernareggi, Clinical pharmacokinetics of nimesulide, Clin Pharmacokinet 35(4) (1998) 247-74.
[76] J.M. Reid, S.J. Mandrekar, E.C. Carlson, W.S. Harmsen, E.M. Green, R.M. McGovern, E. Szabo, M.M. Ames, D. Boring, P.J. Limburg, N. Cancer Prevention, Comparative bioavailability

of sulindac in capsule and tablet formulations, Cancer Epidemiol Biomarkers Prev 17(3) (2008) 674-9.
[77] B.N. Swanson, V.K. Boppana, P.H. Vlasses, G.I. Holmes, K. Monsell, R.K. Ferguson, Sulindac disposition when given once and twice daily, Clin Pharmacol Ther 32(3) (1982) 397-403.
[78] J. Mattila, R. Mantyla, A. Vuorela, U. Lamminsivu, P. Mannisto, Pharmacokinetics of graded oral doses of sulindac in man, Arzneimittelforschung 34(2) (1984) 226-9.
[79] J. Nagelschmitz, M. Blunck, J. Kraetzschmar, M. Ludwig, G. Wensing, T. Hohlfeld, Pharmacokinetics and pharmacodynamics of acetylsalicylic acid after intravenous and oral administration to healthy volunteers, Clin Pharmacol 6 (2014) 51-9.
[80] N. Muir, J.D. Nichols, J.M. Clifford, M.R. Stillings, R.C. Hoare, The influence of dosage form on aspirin kinetics: implications for acute cardiovascular use, Curr Med Res Opin 13(10) (1997) 547-53.
[81] N. Muir, J.D. Nichols, M.R. Stillings, J. Sykes, Comparative bioavailability of aspirin and paracetamol following single dose administration of soluble and plain tablets, Curr Med Res Opin 13(9) (1997) 491-500.
[82] R.H. Rumble, P.M. Brooks, M.S. Roberts, Metabolism of salicylate during chronic aspirin therapy, Br J Clin Pharmacol 9(1) (1980) 41-5.
[83] T.C. Kwong, Salicylate measurement: clinical usefulness and methodology, Crit Rev Clin Lab Sci 25(2) (1987) 137-59.

Figure 1

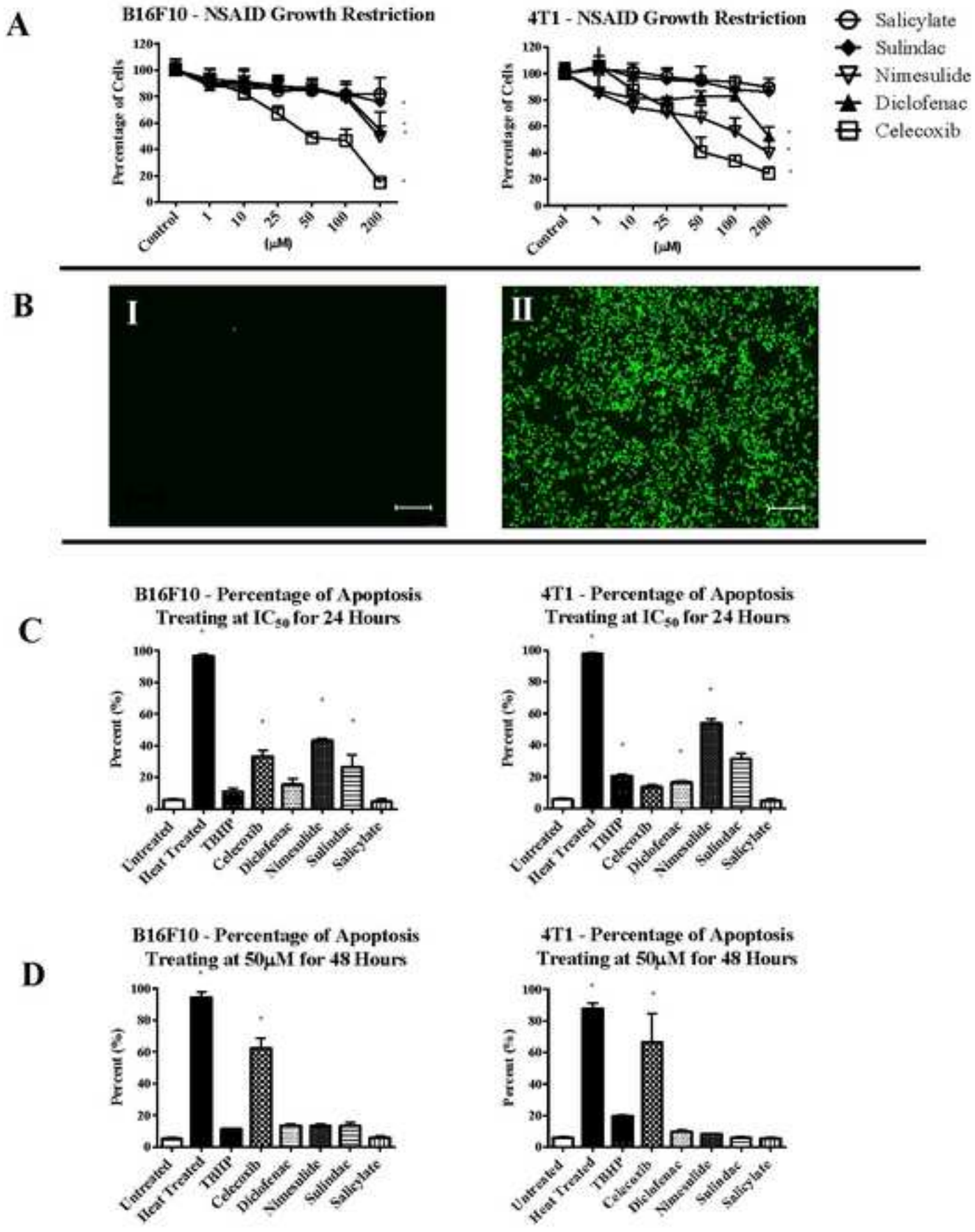

Figure 2

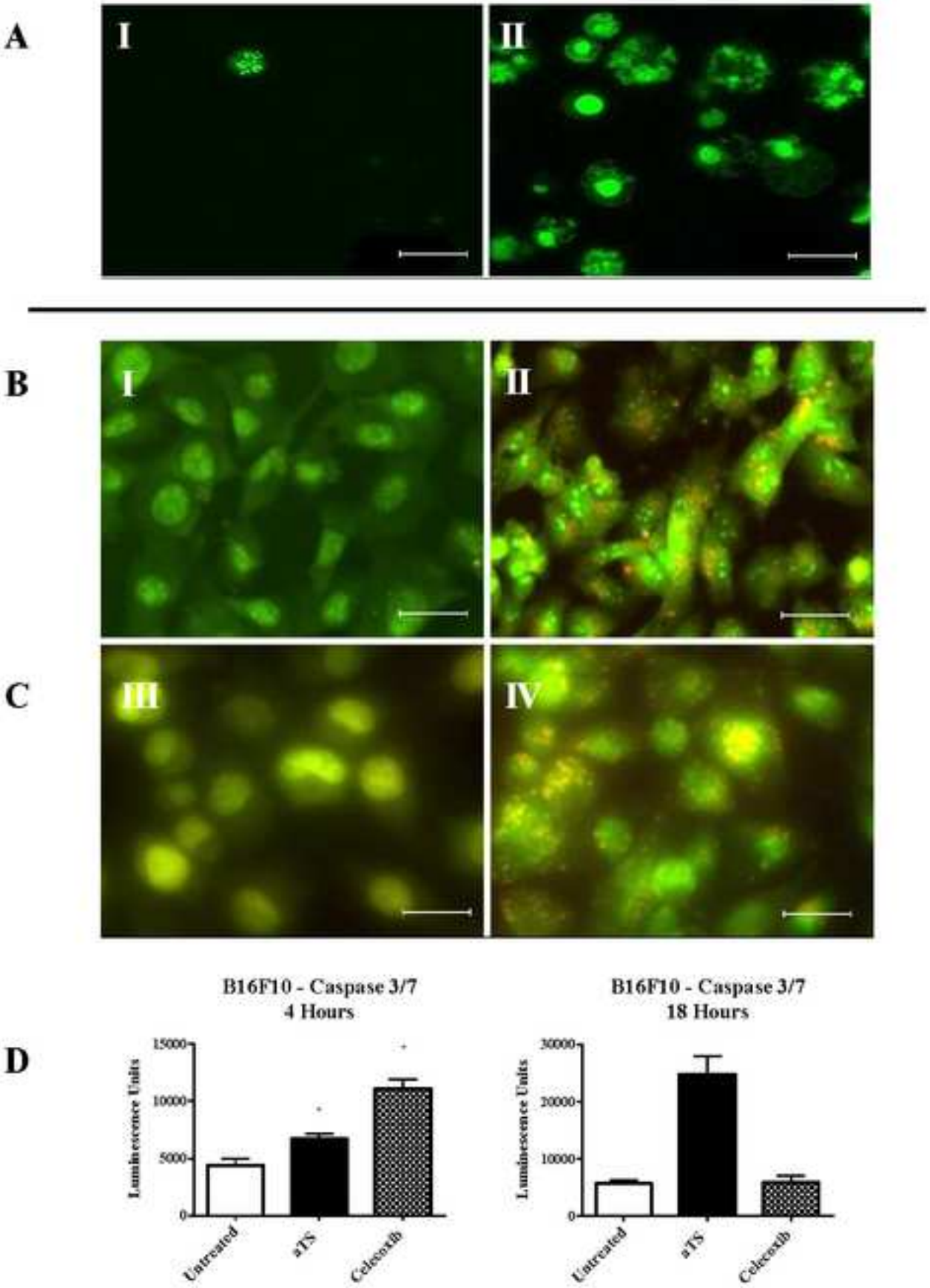
A
I
II
B
I
II
C
III
IV
D
B16F10 - Caspase 3/7
4 Hours
Luminescence Units
15000
10000
5000
0
Untreated
aTS
Celecoxib
B16F10 - Caspase 3/7
18 Hours
Luminescence Units
30000
20000
10000
0
Untreated
aTS
Celecoxib

Figure 3

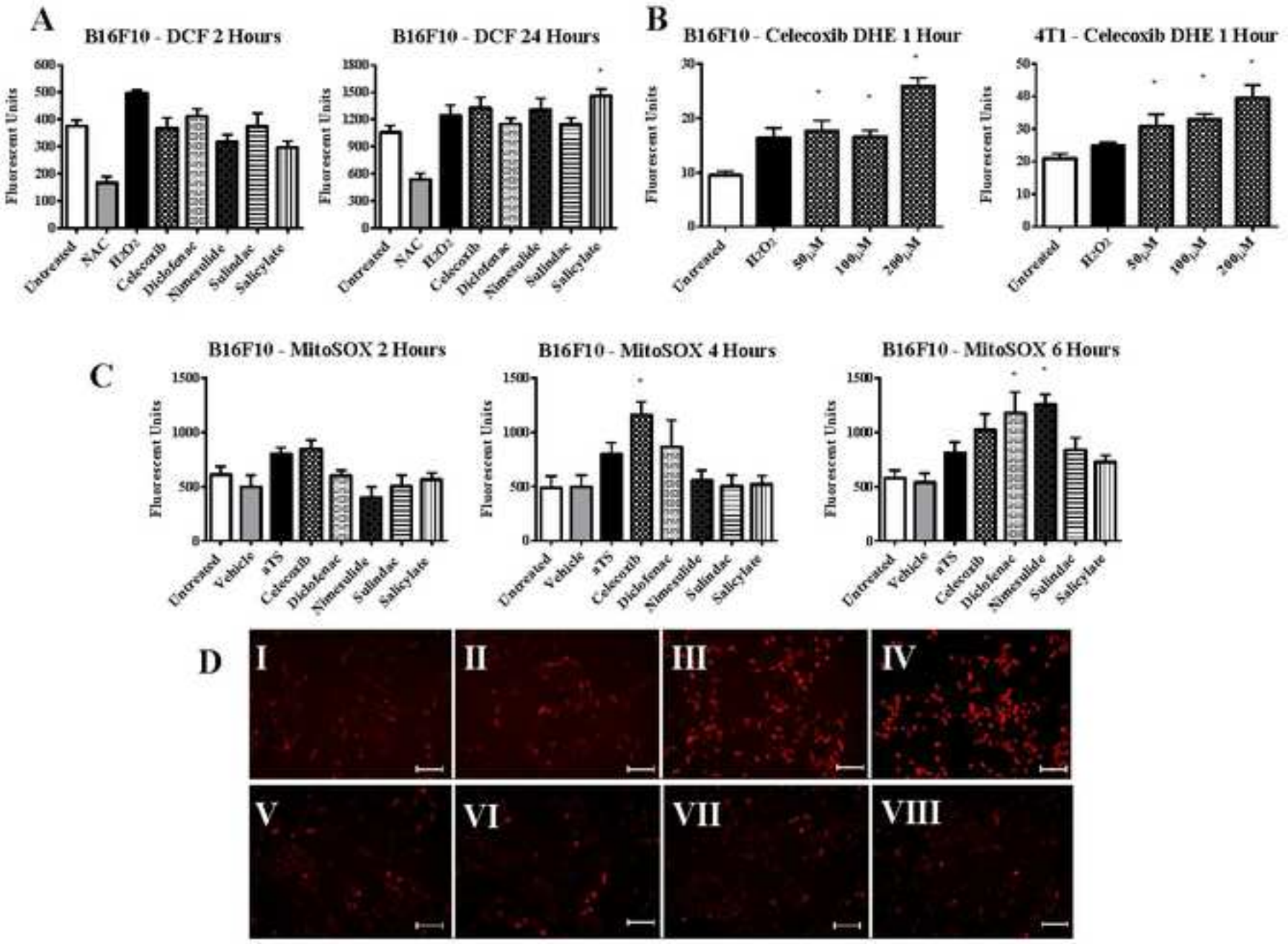

Figure 4

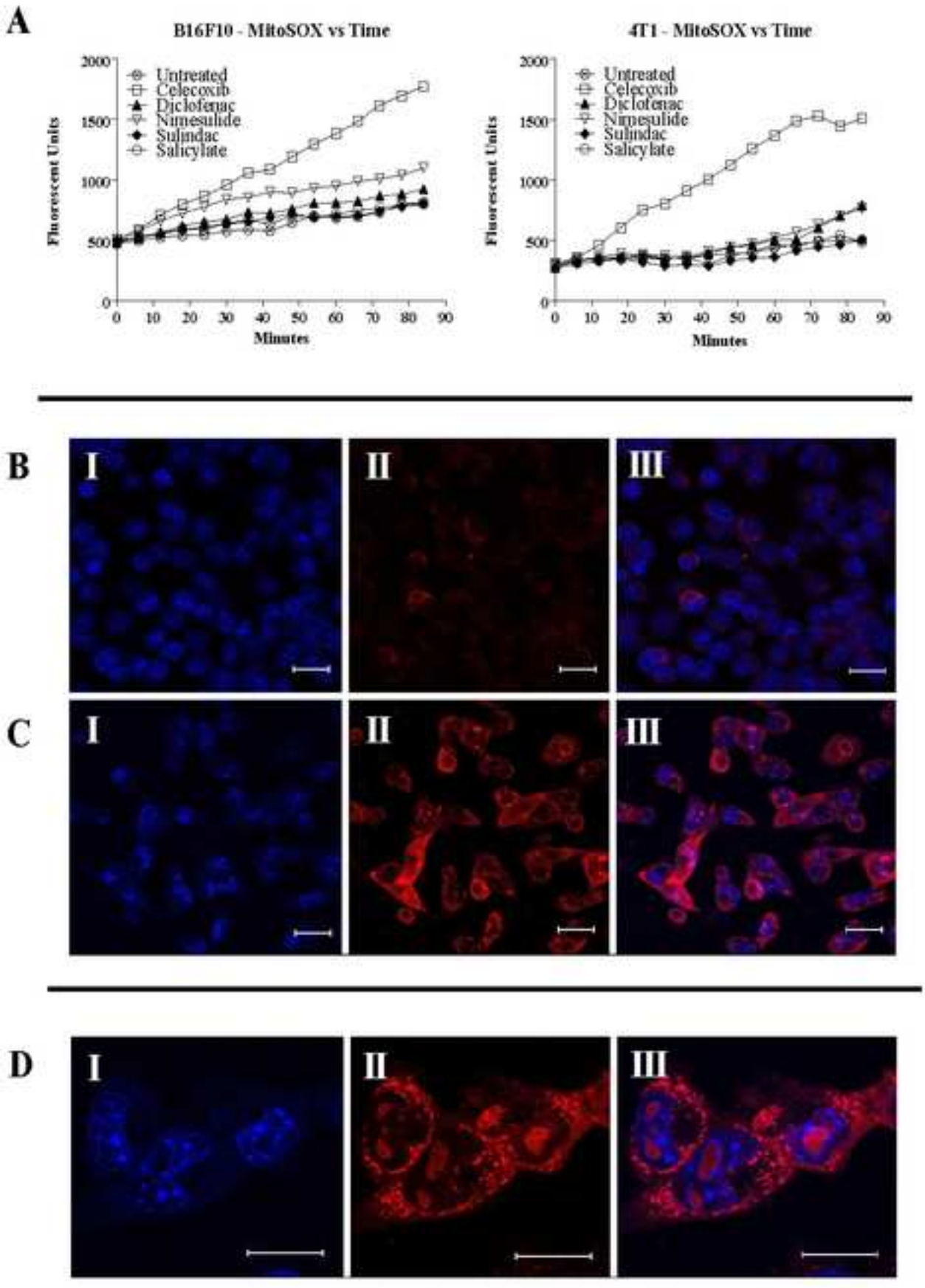
A
B16F10 - MitoSOX vs Time
4T1 - MitoSOX vs Time
Fluorescent Units
Minutes
Untreated
Celecoxib
Diclofenac
Nimesulide
Sulindac
Salicylate
B
C
D
I
II
III

Figure 5

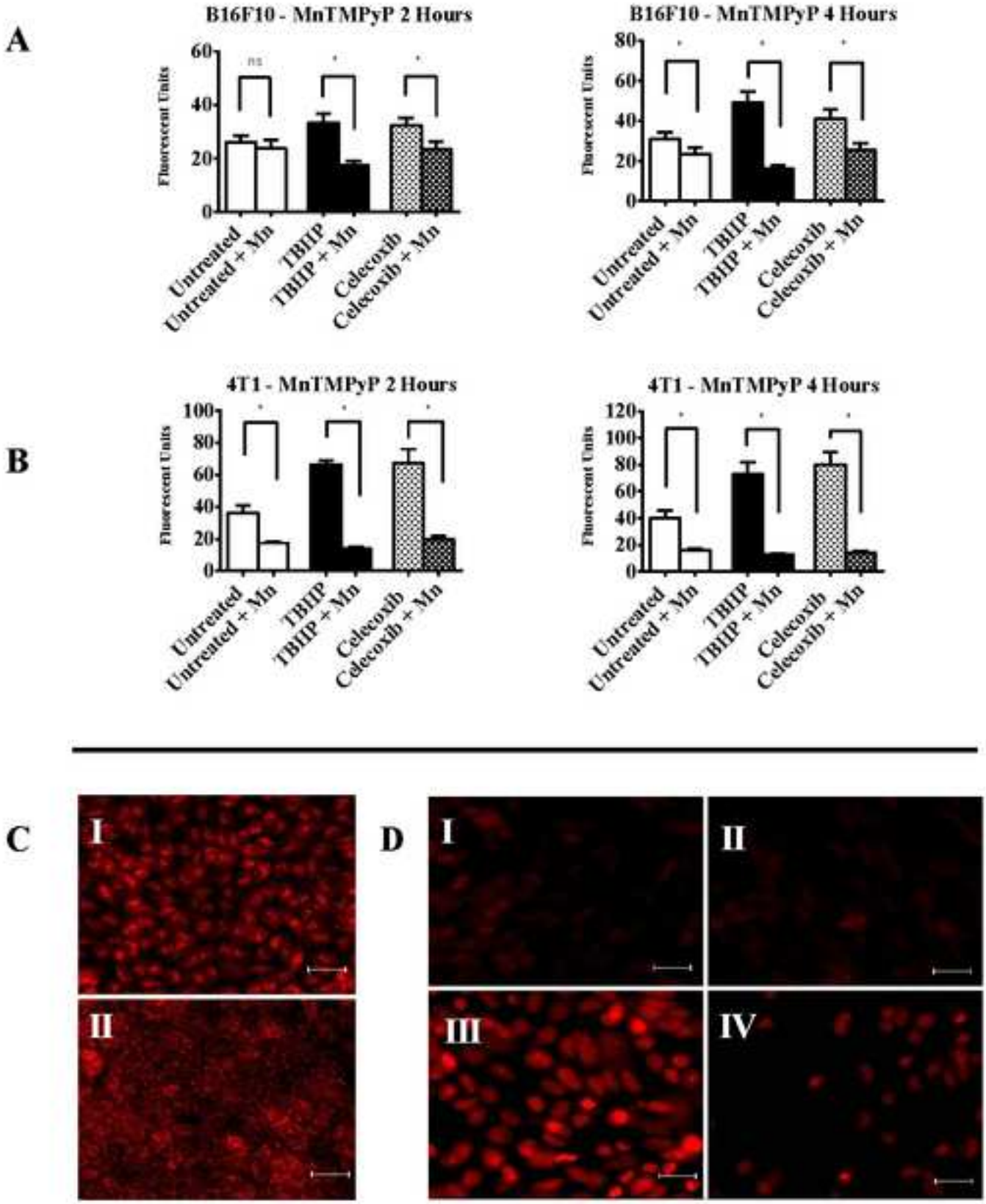

Figure 6

A

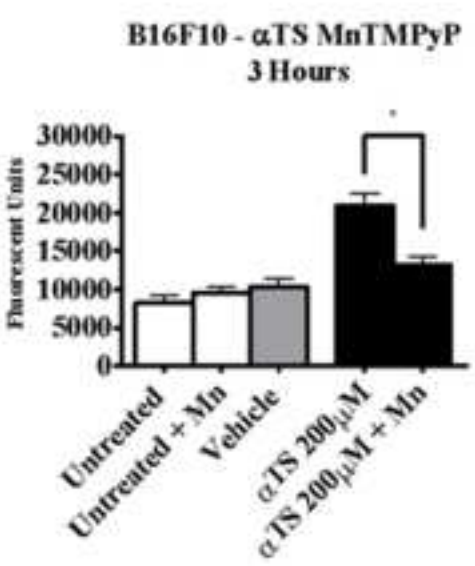
B16F10 - αTS MnTMPyP
3 Hours
Fluorescent Units
30000
25000
20000
15000
10000
5000
0
*
Untreated
Untreated + Mn
Vehicle
αTS 200μM
αTS 200μM + Mn

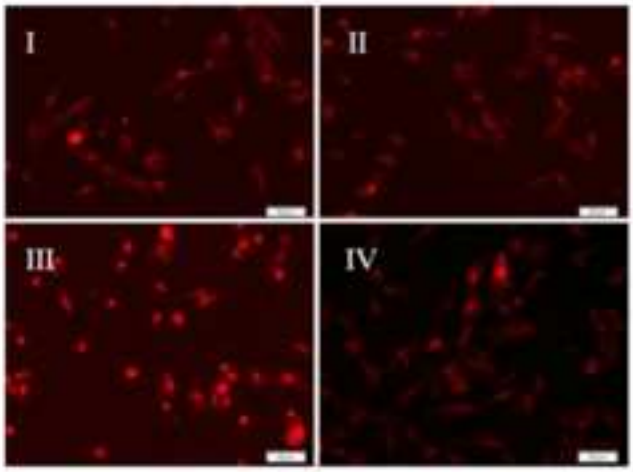
I
II
III
IV

B

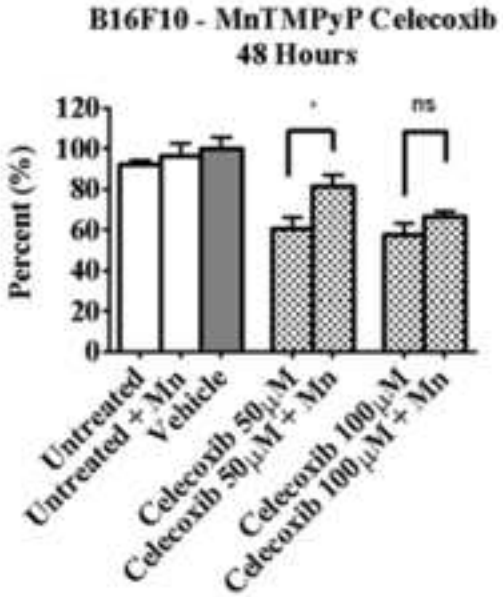
B16F10 - MnTMPyP Celecoxib
48 Hours
Percent (%)
120
100
80
60
40
20
0
*
ns
Untreated
Untreated + Mn
Vehicle
Celecoxib 50μM
Celecoxib 50μM + Mn
Celecoxib 100μM
Celecoxib 100μM + Mn

Figure 7

A

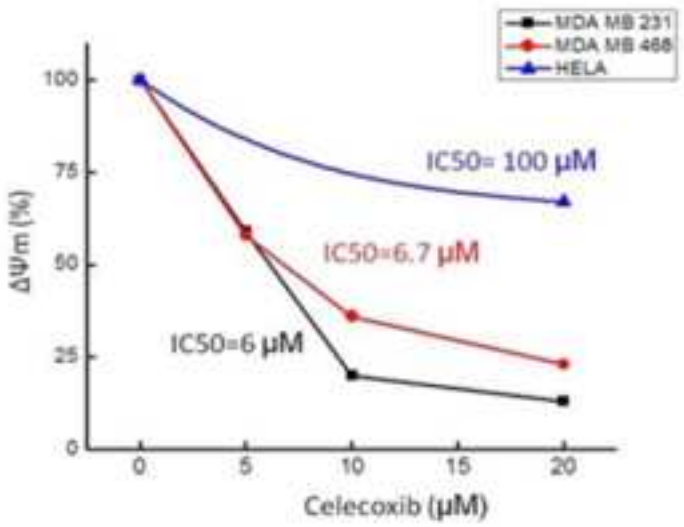
MDA MB 231
MDA MB 468
HELA
IC50= 100 µM
IC50=6.7 µM
IC50=6 µM
ΔΨm (%)
Celecoxib (µM)

B

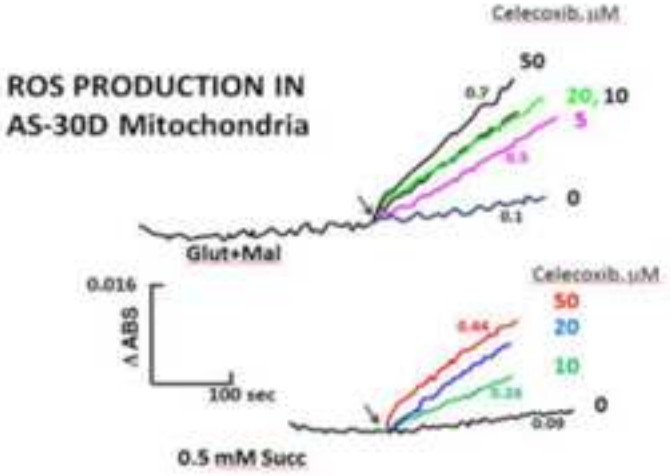
ROS PRODUCTION IN
AS-30D Mitochondria
Celecoxib, µM
Glut+Mal
Celecoxib, µM
Δ ABS
100 sec
0.5 mM Succ

C

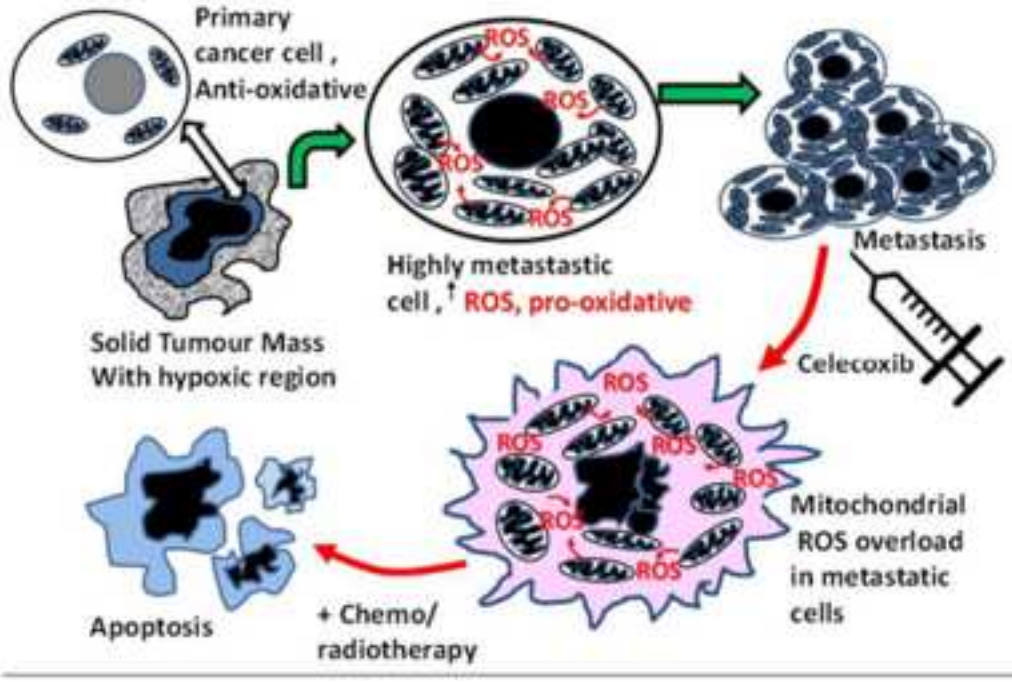
Primary
cancer cell ,
Anti-oxidative
Solid Tumour Mass
With hypoxic region
Highly metastastic
cell , ↑ ROS, pro-oxidative
Metastasis
Celecoxib
Mitochondrial
ROS overload
in metastatic
cells
+ Chemo/
radiotherapy
Apoptosis